AD_____

Award Number: DAMD17-99-1-9088

TITLE: Identification and characterization of novel antimitotic
         compounds for the treatment of breast cancer

PRINCIPAL INVESTIGATOR: Michel Roberge, Ph.D.

CONTRACTING ORGANIZATION: The University of British Columbia
                           Vancouver, British Columbia V6T 1Z3

REPORT DATE: August 2002

TYPE OF REPORT: Final

PREPARED FOR: U.S. Army Medical Research and Materiel Command
                Fort Detrick, Maryland 21702-5012

DISTRIBUTION STATEMENT: Approved for Public Release;
                          Distribution Unlimited

The views, opinions and/or findings contained in this report are
those of the author(s) and should not be construed as an official
Department of the Army position, policy or decision unless so
designated by other documentation.

REPORT DOCUMENTATION PAGE

1. AGENCY USE ONLY (Leave blank)	2. REPORT DATE August 2002	3. REPORT TYPE AND DATES COVERED Final (15 Jul 99 – 15 Jul 02)

4. TITLE AND SUBTITLE
Identification and characterization of novel antimitotic compounds for the treatment of breast cancer

5. FUNDING NUMBERS
DAMD17-99-1-9088

6. AUTHOR(S)
Michel Roberge, Ph.D.

7. PERFORMING ORGANIZATION NAME(S) AND ADDRESS(ES)
The University of British Columbia
Vancouver, British Columbia V6T 1Z3

E-Mail: michel@otter.biochem.ubc.ca

8. PERFORMING ORGANIZATION REPORT NUMBER

9. SPONSORING / MONITORING AGENCY NAME(S) AND ADDRESS(ES)
U.S. Army Medical Research and Materiel Command
Fort Detrick, Maryland 21702-5012

10. SPONSORING / MONITORING AGENCY REPORT NUMBER

20030122 111

11. SUPPLEMENTARY NOTES

12a. DISTRIBUTION / AVAILABILITY STATEMENT
Approved for Public Release; Distribution Unlimited

12b. DISTRIBUTION CODE

13. ABSTRACT (Maximum 200 Words)

Our goal was to find new antimitotic drugs for the treatment of breast cancer using a novel cell-based assay to screen natural product libraries and guide the purification of their active components.

We carried out a screen of over 30,000 extracts of terrestrial plants, algae and marine organisms, obtained 223 positive extracts, and isolated and identified active compounds from several of the positive extracts.

We isolated a new rhizoxin analog, two paclitaxel analogs, three flavonoids, as well as agents that do not target microtubules, such as okadaic acid analogs, 3'-acetoxychavicol acetate, vernonataloide and 13-hydroxy-15-oxozoapatlin.

We also isolated new analogs of the microtubule-stabilizing compound eleutherobin and produced several more by synthetic transformation. We used the analogs to carry out an extensive structure-activity relationship study of eleutherobin and identified unanticipated structural requirements that will be important for future pharmacophore models. We have been able to isolate eleutherobin from the producing octocoral grown in aquaculture, providing a renewable resource for this natural product in quantities sufficient for preclinical testing.

14. SUBJECT TERMS
breast cancer, antimitotic drugs, cell-based assay

15. NUMBER OF PAGES
40

16. PRICE CODE

17. SECURITY CLASSIFICATION OF REPORT	18. SECURITY CLASSIFICATION OF THIS PAGE	19. SECURITY CLASSIFICATION OF ABSTRACT	20. LIMITATION OF ABSTRACT
Unclassified	Unclassified	Unclassified	Unlimited

Table of Contents

INTRODUCTION

Antimitotics are drugs that kill cancer cells by causing them to arrest in mitosis. Antimitotics currently used in breast cancer therapy include paclitaxel, vincristine and vinblastine. Although these drugs are extremely valuable, they are not ideal because they have serious side effects, and, most importantly, many breast cancers are resistant to them. Our goal was to find new antimitotic drugs for the treatment of breast cancer using a novel cell-based assay to screen natural product libraries and guide the purification of their active components.

BODY

TASK 1

Screen the natural product collection (5,000 extracts) for antimitotic activity (months 1-4)

In Year 1 we completed a screen of about 30,000 extracts. In addition to the proposed collection of marine microorganisms, we also screened two other collections in order to maximize the diversity of sources of antimitotics. One was of marine invertebrates collected by the Andersen laboratory from a variety of habitats: cold temperate Pacific Ocean waters along the coast of British Columbia, tropical Pacific Ocean reefs off Motupore and Madang in Papua New Guinea, tropical waters off the island of Dominica in the Caribbean, and temperate Atlantic waters surrounding the Isle of Man (U.K.). The second collection was obtained from the Natural Products Repository of the National Cancer Institute Developmental Therapeutics Program. It is a diverse collection of terrestrial plants, algae and marine organisms from around the world. Access to this valuable collection was granted in January 1999.

To deal with the massive amount of screening, we adapted our original ELISA assay which is a moderately lengthy and labor-intensive procedure requiring the preparation of cell lysates, their transfer to protein-binding plates, and many solution changes. We simplified it, reducing the time of the procedure and the number of steps by half and avoiding transfer of samples to ELISA plates. In the new procedure, the cells are fixed with formaldehyde in the microtiter culture plate and permeablized with methanol and detergents, and the TG-3 primary antibody and HRP-conjugated secondary antibody are added simultaneously. Colorimetric detection of HRP activity remains unchanged. Since cell fixation and permeabilization *in situ* are steps commonly used in immunocytochemistry, we termed the assay Enzyme-Linked Immuno-Cytochemical Assay or ELICA.

In order to handle the large amount of data being generated by our screen, we developed a database for all the positive extracts. The database lists each extract's date of screening, its storage location, identifying number, its source (marine invertebrate, plant, or alga), its family, genus and species, and notes concerning the stage of purification and/or characterization it has undergone. The database may be searched by any of these

4

parameters. We have found the database to be particularly useful when prioritizing extracts to undergo chemical purification. For example, positive extracts from organisms of the same genus, such as the plants *Ilex siderioxyloides* and *Ilex macrophylla* are very likely to contain the same or similar antimitotics. Only one would be selected for further intensive study when searching for structurally novel compounds. Similarly extracts from organisms in the same genus as an organism known to contain an identified antimitotic would be a low priority for further study. For example, the positive extract of *Combretum fuscum* is very likely to contain the known antimitotic combretastatin originally identified in *Combretum caffrum* (Sackett, 1993). Conversely, in order to find new analogs of a particularly important antimitotic, extracts from related organisms may be selected. We took this approach for finding new analogs of eleutherobin, and selected extracts from organisms related to *Erythropodium caribaeorum* for futher study. The significance of this choice is detailed under Task 2.

The original ELISA assay, the modified ELICA assay, and the screen of the first 25,000 extracts was published in Cancer Research (Roberge et al., 2000; Appendix 1).

TASK 2
Isolate and identify the chemical structure of active compounds (months 5-30)

The pilot study we presented in our proposal yielded two antimitotics out of 263 screened, a hit rate of 0.7%. Our final screen gave us 223 positive extracts out of 30,000 screened, also a hit rate of 0.7%. The process of fractionation, dereplication, purification and chemical structure elucidation of active compounds has been completed for selected positive extracts. Their structural formulae are shown in Figures 1 and 2.

We found a new rhizoxin analog from a *Pseudomonas* species (Roberge et al., 2000; Appendix 1) and two paclitaxel analogs in the stem bark of the tree *Ilex macrophylla* (Roberge et al., 2000; Appendix 1). From a plant extract we isolated 3 active flavonoids (3'-methoxycalycopterin, 4',5,7-trihydroxy-3,3',6,8-tetramethoxyflavone, 3,3'dimethoxyquercaetin) and one inactive analog. From a marine invertebrate, we isolated 2 okadaic acid analogs, 27-O-acyl-dinophysistoxin and 27-O-acyl-okadaic acid. We also isolated 3'acetoxychavicol acetate, vernonataloide, and 13-hydroxy-15-oxozoapatlin from different plants.

We discovered a new source of eleutherobin in the octocoral *Erythropodium caribaeorum* from which we purified six new eleutherobin analogs (Cinel, 2000a; Appendix 1). We pursued this further, obtaining 12 positive extracts from corals related to *Erythropodium caribaeorum* that we suspected might contain other eleutherobin analogs. From these, we completed the isolation and identification of four additional analogs (Britton et al., 2001a; Appendix 1). We produced several other analogs by synthetic transformation (Britton et al., 2001b; Appendix 1). We also demonstrated that the eleutherobin initially described by Fenical and coworkers (Lindel et al., 1997) is an
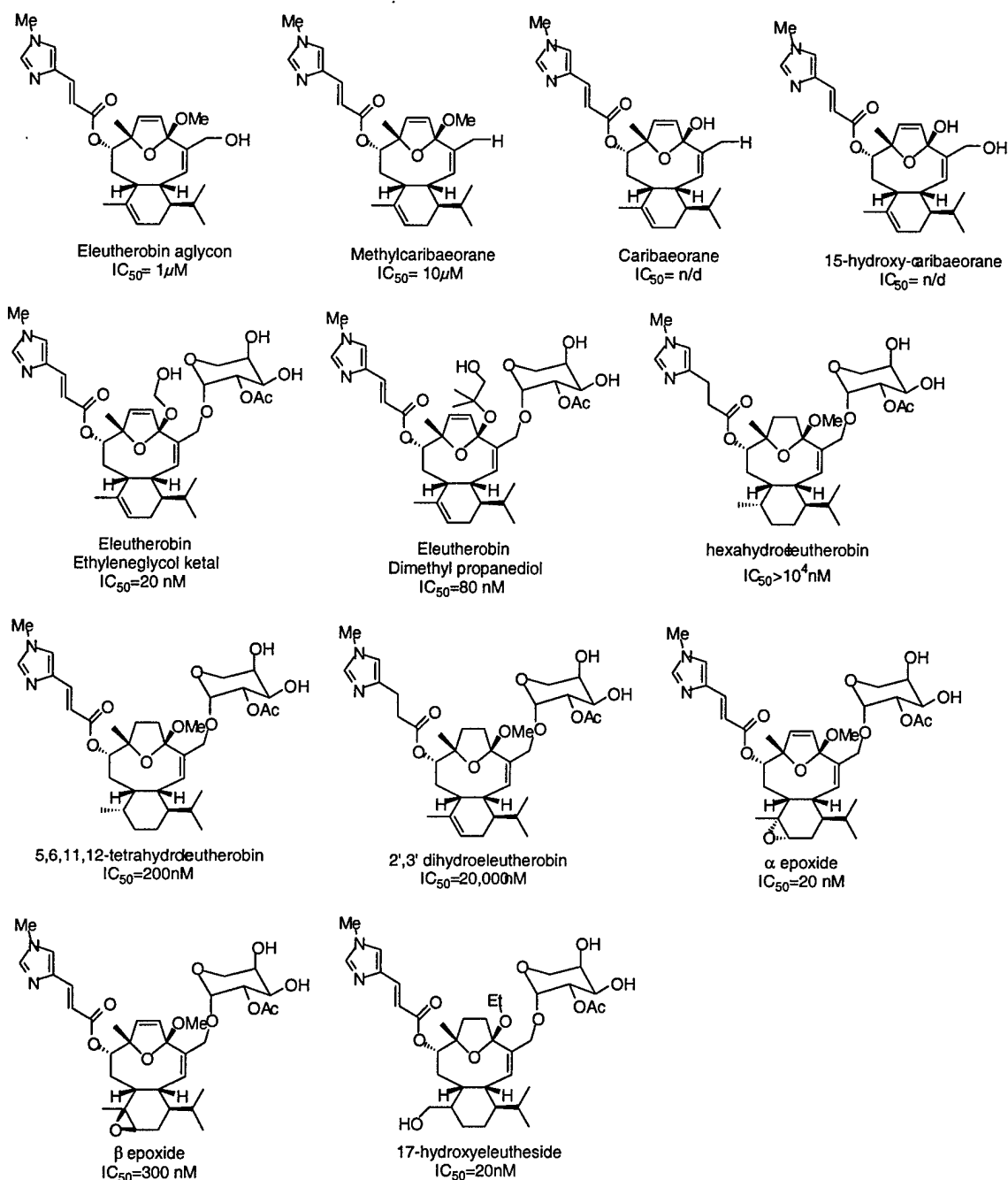
5

Figure 1. Structural formulae of eleutherobin analogs purified or synthesized and their IC_{50} for mitotic arrest.

isolation artifact and that desmethyleleutherobin (first described by us in Year 1) is the natural product (Britton et al, 2001a; Appendix 1). Most importantly, we have now succeeded in isolating active eleutherobin compounds from cultured *Erythropodium caribaeorum*, thus providing a renewable resource for this natural product (Tagliatela-Scarfati, 2002; Appendix 1).
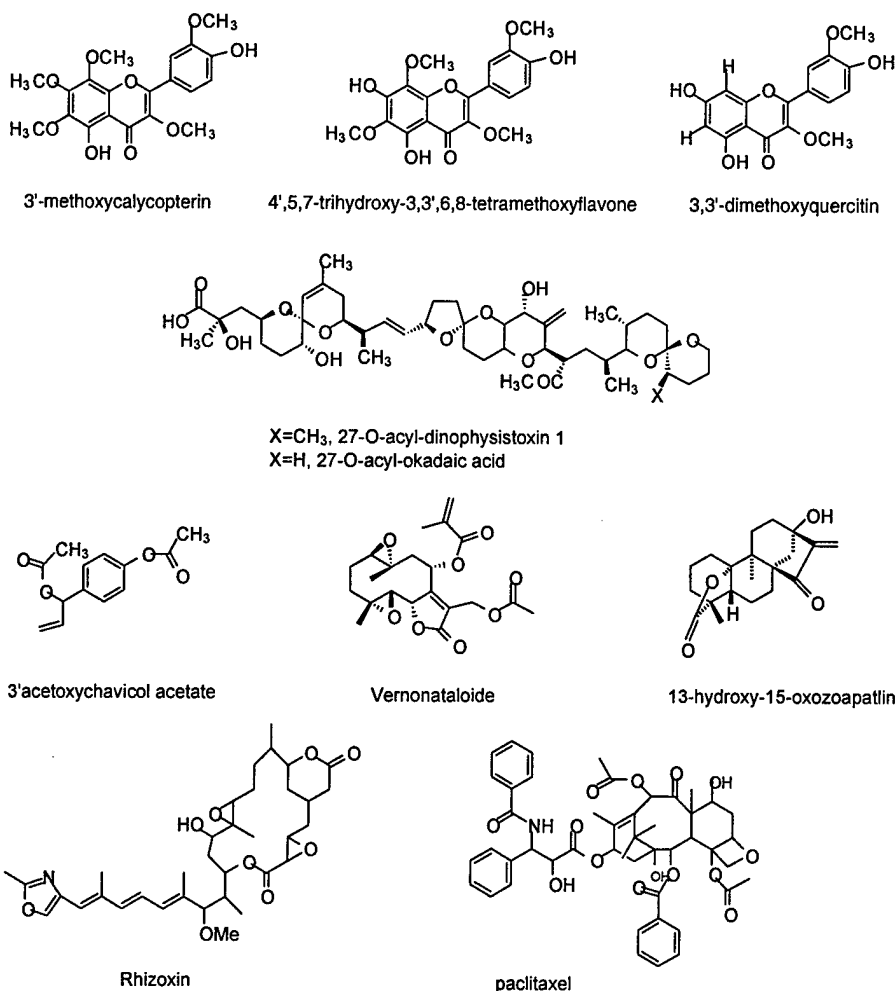
Figure 2. Structural formulae of non-eleutherobin antimitotics.

TASK 3

Mechanism of action of new antimitotic compounds (months 13-32)

We used several assays to investigate the mechanism of action of our purified antimitotics. The first assay examined the effect of the compounds on cells. Cells grown on coverslips were treated with the compounds, and examined by immunofluorescence microscopy using the DNA dye bisbenzimide to visualize the chromosomes and a monoclonal antibody to β-tubulin to examine the microtubules of interphase cells and the spindle of mitotic cells. A second assay examined whether the compounds can interact directly with purified tubulin to cause either its depolymerization or its polymerization. A third assay examined whether the antimitotic effect of the compounds is due to inhibition of Ser/Thr protein phosphatases. In a 96-well format phosphatases, either in crude extract form or as purified protein phosphatase 1A or 2A, and a phosphopeptide substrate are

7

incubated with the antimitotic compound and inhibition of release of phosphate is detected by decreased malachite green signal.

The flavonoids caused the cells to arrest in mitosis with depolymerized microtubules. This is the most common mechanism of action for antimitotics. The IC_{50} of the most active analog was about 10 μg/ml. These compounds belong to a family of flavones related to centaureidin whose antimitotic properties have been extensively studied (Beutler et al., 1998).

The okadaic acid analogs did not cause microtubule bundling or depolymerization in the cell-based tubulin immunofluorescence assay. However they were potent inhibitors of Serine/Threonine protein phosphatases (IC_{50} 0.3 ng/ml).

3'acetoxychavicol acetate and vernonataloide did not cause microtubule bundling or depolymerization. In fact treated cells, although rounded up, had none of the other standard morphological features of mitotic cells i.e. the chromosomes were not condensed, there was no mitotic spindle, and the nuclear lamina remained intact. However, further study showed that at the biochemical level treated cells had undergone many proline-directed phosphorylation events strictly associated with mitosis, such as phosphorylation of histone H3 at Ser10, phosphorylation of nucleolin at the TG3-immunoreactive site, phosphorylation of GF-7 antigen, and phosphorylation of MPM2 antigens. This strongly suggests that these two compounds are activating a proline-directed kinase. They did not act as Serine/Threonine phosphatase inhibitors. We are now carrying out biochemical studies to determine the kinase involved and its mechanism of activation.

13-hydroxy-15-oxozoapatlin caused cells to arrest in mitosis (IC_{50} 10 μM), but with an unusual morphology not produced by other antimitotics: their chromosomes were condensed and a mitotic spindle was formed, but the chromosomes failed to align properly on the mitotic spindle. It was also able to act as a G2 checkpoint inhibitor, i.e. it released cells from arrest in G2 phase of the cell cycle following DNA damage and caused them to enter mitosis (Rundle, 2001). This interesting combination of effects suggests a novel mechanism of action and we are now pursuing the identification of the relevant targets.

The new eleutherobin analogs all arrest cells in mitosis with bundled microtubules. Using the in vitro tubulin assay confirmed that the bundling of microtubules observed in cells is caused by a direct interaction between the eleutherobins and tubulin.

In addition, we used our cell-based antimitotic assay to quantitatively compare the antimitotic activity of the different analogs of rhizoxin, paclitaxel, and eleutherobin, permitting us to determine which regions of these compounds are important for antimitotic activity (Roberge et al., 2000 and Cinel et al., 2000a; Appendix 1). We have also been able to determine the solution and crystal structures of eleutherobin (Cinel,

8

2000b; Appendix 1) and to obtain a refined solution structure of eleutherobin (Cornett et al., submitted). This information is very useful for further drug development. The interpretation and significance of these results for the development of a tubulin-binding pharmacophore for compounds that stabilize microtubules is presented in (Britton et al., 2001b; Appendix 1).

TASK 4
Initial studies on therapeutic potential (months 14-36)

The purified compounds were tested for their ability to inhibit the proliferation of MCF-7mp53 breast cancer cells and of multidrug-resistant MCF-7 cells.

The okadaic acid analogs were found to be very potent inhibitors of proliferation (IC_{50} 1 ng/ml) and were considered likely to be too toxic for therapeutic applications. The flavonoids were not studied further since they are members of a family of compounds extensively studied by others (Beutler, 1998).

3'acetoxychavicol acetate, vernonataloide, and 13-hydroxy-15-oxozoapatlin inhibit proliferation at low micromolar concentrations.

The eleutherobin analogs were particularly promising. Their effectiveness as antimitotics was closely correlated with their ability to inhibit cell proliferation, desmethyleleutherobin and eleutherobin being the most active, with an IC_{50} for inhibition of proliferation of about 18 nM.

A major challenge with products isolated from marine invertebrate sources is to produce sufficient amounts of compound for the animal studies required for drug development. Harvesting large numbers of specimens from the wild is environmentally unsound and costly. Although two elegant syntheses of eleutherobin have been reported, the amounts generated have not been sufficient for testing in animals. We have found that *Erythropodium caribaeorum* grown in aquaculture produces eleutherobin in amounts comparable to those collected in the wild (0.8 mg eleutherobin/100g wet weight) (Tagliatela-Scafati, 2002; Appendix 1). We now have sufficient purified eleutherobin to initiate animal studies.

KEY RESEARCH ACCOMPLISHMENTS

- We have developed the ELICA, a modification of our original assay, which is faster, less labor-intensive and less costly.

- We have completed the purification and identification of active compounds from several positive extracts, including analogs of rhizoxin, paclitaxel, okadaic acid and eleutherobin, as well as the flavonoids 3'-methoxycalycopterin, 4',5,7-trihydroxy-

3,3',6,8-tetramethoxyflavone, 3,3'dimethoxyquercaetin, and the novel antimitotics 3'acetoxychavicol acetate, vernonataloide, and 13-hydroxy-15-oxozoapatlin.

- We have examined the activity of the purified compounds. The flavonoids belong to a recently described family of antimitotics (Beutler, 1998) that act by depolymerizing microtubules. The okadaic acid analogs act through inhibition of Ser/Thr phosphatases but were deemed potentially too toxic for therapeutic use. 3'acetoxychavicol acetate, vernonataloide and 13-hydroxy-15-oxozoapatlin had novel mechanisms of action currently under further study. This success rate for novelty is in part attributable to our efforts at secondary screening of crude extracts to optimize for novelty, implemented in Year 1.

- We have purified a number of different eleutherobin analogs and produced several more by synthetic transformation. This has allowed us to carry out an extensive structure-activity study, using our ELICA assay, that has revealed some striking and unanticipated features of its antimitotic properties. A detailed understanding of the structural requirements for binding of microtubule-stabilizing agents to tubulin is an important tool for the rational design of new microtubule-stabilizing drugs.

- We have determined the solution and crystal structures of eleutherobin which will be useful for further drug development.

- We have been able to isolate active eleutherobin from *Erythropodium caribaeorum* grown in aquaculture. This renewable resource has permitted the purification of sufficient compound to make possible the testing of anticancer activity in experimental tumors in mice in the immediate future.

REPORTABLE OUTCOMES
Publications (copies provided in Appendix 1)

1. Roberge, M., Cinel, B., Anderson, H. J., Lim, L., Jiang, X., Xu, L., Kelly, M. T. and Andersen, R. J. (2000). Cell-based screen for antimitotic agents and identification of new analogs of rhizoxin and eleutherobin. Cancer Res. 60: 5052-5058.

2. Cinel B, Roberge, M. Behrisch, H. and van Ofwegen, L. (2000a). Antimitotic diterpenes from *Erythropodium caribaeorum* test pharmacophore models for microtubule stabilization. Org. Lett. 2, 257-260.

3. Cinel B, Patrick BO, Roberge M and Andersen RJ (2000b). Solid-state and solution conformations of eleutherobin obtained from X-ray diffraction analysis and solution NOE data. Tetrahedron Letters 41, 2811-2815.

4. Britton, R., Roberge, M., Berisch, H. and Andersen, R. J. (2001a). Antimitotic diterpenoids from *Erythropodium caribeaorum*: isolation artifacts and putative biosynthetic intermediates. Tetrahedron Lett. 43: 2953-2956.

5. Britton, R., de Silva, E. D., Bigg, C. M. , McHardy, L. M., Roberge, M. and Andersen, R. J. (2001b). Synthetic transformations of eleutherobin reveal new features of its microtubule-stabilizing pharmacophore. J. Am. Chem. Soc. 123:8632-8633.

6. Tagliatela-Scafati, O., Campbell, M., Roberge, M. and Andersen, R. J. (2002). Diterpenoids from cultured *Erythropodium caribaeorum*. Submitted to J. Am. Chem. Soc.

Patents

"Antimitotic compounds from Marine Organisms", Canada filed 11.24.1999; PCT filed 11.24.2000; USA filed 06.22.2001.

CONCLUSIONS

Our cell-based assay for antimitotics met our expectations. It revealed 223 positive extracts from 30,000 extracts screened, and permitted us to purify the active compounds, even as very minor components, from those selected for further investigation. Several of these compounds are novel antimitotics. The assay also permitted us to carry out extensive structure-activity relationship studies using the different analogs we have purified, an essential part of drug development.

Of immediate value to breast cancer treatment is that our research has revealed a renewable source of the compound eleutherobin which should provide sufficient material for preclinical and early phase clinical trials of this promising compound.

REFERENCES

Beutler J.A., Hamel E., Vlietinck A.J., Haemers A., Rajan P., Roitman, J.N., Cardellina J.H. and Boyd M.R. (1998). Structure-activity requirements for flavone cytotoxicity and binding to tubulin. J. Med Chem. 41, 2333-2338.

Cornett, B., Monteagudo, E., Cicero, D. O., Cinel, B., Andersen, R. J., Roberge, M., Liotta, D. C. and Snyder, J. P. Conformational analysis of the microtubule-stabilizing agent eleutherobin in CDCl$_3$. (Submitted).

Lindel T., Jensen P.R., Fenical W., Long B.H., Casazza A.M., Carboni J and Fairchild C.R. (1997). Eleutherobin, a new cytotoxin that mimics paclitaxel (Taxol) by stabilizing microtubules. J. Am. Chem. Soc. 119, 8744-8745.

Rundle, N., Xu, L., Andersen, R. J. and Roberge, M. (2001). G2 DNA damage checkpoint inhibition and antimitotic activity of 13-hydroxy-15-oxozoapatlin. J. Biol. Chem. 276:48231-48236.

Sackett DL (1993). Podophyllotoxin, steganacin and combretastatin: natural products that bind at the colchicine site of tubulin. Pharmacol. Ther. 59, 163-228.

APPENDIX 1

Manuscripts and published papers arising from research supported by this grant.

Cell-based Screen for Antimitotic Agents and Identification of Analogues of Rhizoxin, Eleutherobin, and Paclitaxel in Natural Extracts[1]

Michel Roberge,[2] Bruno Cinel, Hilary J. Anderson, Lynette Lim, Xiuxian Jiang, Lin Xu, Cristina M. Bigg, Michael T. Kelly, and Raymond J. Andersen

Department of Biochemistry and Molecular Biology, University of British Columbia, Vancouver, British Columbia, V6T 1Z3 Canada [M. R., H. J. A., L. L., X. J., C. M. B.]; Departments of Chemistry and Oceanography (EOS), University of British Columbia, Vancouver, V6T 1Z1 Canada [B. C., L. X., R. J. A.]; and SeaTek Marine Biotechnology, Inc., Surrey, British Columbia, V4A 7M4 Canada [M. T. K.]

ABSTRACT

We describe a cell-based assay for antimitotic compounds that is suitable for drug discovery and for quantitative determination of antimitotic activity. In the assay, cells arrested in mitosis as a result of exposure to antimitotic agents in pure form or in crude natural extracts are detected by ELISA using the monoclonal antibody TG-3. The assay was used to screen >24,000 extracts of marine microorganisms and invertebrates and terrestrial plants and to guide the purification of active compounds from 5 of 119 positive extracts. A new rhizoxin analogue was found in a *Pseudomonas* species, six new eleutherobin analogues were identified from the octocoral *Erythropodium caribaeorum*, and two paclitaxel analogues were found in the stem bark of the tree *Ilex macrophylla*. The assay was also used for quantitative comparison of the antimitotic activity of different analogues. It revealed the importance of the C-11 to C-13 segment of the diterpene core of eleutherobin for its antimitotic activity. The identification of antimitotic compounds in very low abundance and their high (0.5%) occurrence in natural extracts indicates that drug discovery efforts using this cell-based assay may lead to the identification of structurally novel antimitotic agents.

INTRODUCTION

Antimitotic agents are compounds that arrest cells in mitosis. Several are clinically important anticancer drugs, including the *Vinca* alkaloids vinblastine, vincristine, and vinorelbine (1) and the taxanes paclitaxel and docetaxel (2). They cause mitotic arrest by interfering with the assembly or disassembly of α- and β-tubulin into microtubules. At high concentrations, the *Vinca* alkaloids and most other antimitotics cause complete microtubule depolymerization, whereas the taxanes cause bundling of microtubules by stabilizing them against depolymerization. At low concentrations, neither depolymerization nor bundling is observed, but there is sufficient alteration in the dynamics of tubulin loss or addition at the ends of mitotic spindle microtubules to prevent the spindle from carrying out its function of attaching to and segregating the chromosomes, and cells arrest in mitosis (3, 4). Prolonged arrest eventually leads to cell death, either in mitosis or after an eventual escape from mitotic arrest (5, 6). Another class of antimitotic agents, represented by estramustine, does bind tubulin (7) but may also bind microtubule-associated proteins and prevent them from regulating interactions between tubulin polymers (8). Agents that are not known to interact with microtubules, such as inhibitors of protein phosphatases 1 and 2A and mitotic kinesin inhibitors, can also arrest cells in mitosis (9–11).

The *Vinca* alkaloids were isolated from the periwinkle plant, which originally attracted attention because of reported hypoglycemic properties. However, periwinkle extracts showed no antidiabetic action but were found to prolong the life of mice bearing a transplantable lymphocytic leukemia (1). This led to the identification of vincristine and vinblastine. Paclitaxel was isolated from the bark of the Pacific yew tree, an extract of which showed antineoplastic activity in the NCI[3] large-scale screen (2). Vinorelbine and docetaxel are semisynthetic analogues.

These drugs, although extremely valuable, are not ideal. They have numerous toxicities, principally myelosuppression and neurotoxicity. More importantly, many cancers are inherently resistant to these drugs or become so during prolonged treatment (1, 2). This is often the result of multidrug resistance caused by overexpression of P-glycoprotein, which functions as a drug efflux pump. Other sources of resistance include increased expression of tubulin isotypes to which a particular drug binds less effectively and alterations in α- and β-tubulin structure, by mutation or posttranslational modification, that reduce binding.

Antimitotics with different chemical structures might show increased specificity to mitotic microtubules rather than neuronal microtubules and reduce unwanted side effects and might be effective against resistant cancers. Many other antimitotics have been discovered, some of which show promise in preclinical studies or have entered clinical trials (12). However, they were discovered either by serendipity or by cytotoxicity screening, or because they showed patterns of cytotoxic activity against panels of cancer cell lines similar to patterns shown by other antimitotic agents (13). The search for better antimitotics would be greatly aided by rational assays for use in drug screens.

We have developed a rapid and reliable cell-based screen for antimitotic agents. In this report, we describe the assay, its application to a screen of >24,000 natural extracts, and the purification and characterization of paclitaxel analogues and new rhizoxin and eleutherobin analogues.

MATERIALS AND METHODS

Cell Culture and Treatment. Human breast carcinoma MCF-7 cells were cultured as monolayers (14). The cells were seeded at 10,000/well of 96-well polystyrene tissue culture plates (Falcon) in 100 μl of medium and were allowed to grow overnight. Crude extracts were then added at about 10 or 1 μg/ml from 1000-fold stocks in DMSO. Untreated samples received an equivalent amount of DMSO and served as negative controls. Cells treated with 100 ng/ml nocodazole (Sigma), from a 1000-fold stock in DMSO, served as positive controls. Cells were incubated for 16–20 h. The relative number of cells in mitosis was then determined by microscopy (14), by ELISA, or by ELICA (see below).

ELISA of Mitotic Cells. After incubation with extracts, the cell culture medium was withdrawn carefully using a pipettor. This did not result in any loss of the rounded-up mitotic cells, which remained attached to the plates. The cells were lysed by adding 100 μl of ice-cold lysis buffer (1 mM EGTA, pH

7.4, 0.5 mM phenylmethylsulfonyl fluoride) and by pipetting up-and-down 10 times. The cell lysates were transferred to 96-well PolySorp plates (Nunc) and dried completely in a stream of air at about 37°C from a hair dryer. Vacant protein binding sites were blocked by adding 200 μl/well of antibody buffer [10 mM Tris-HCl (pH 7.4), 150 mM NaCl, 0.1 mM phenylmethylsulfonyl fluoride, and 3% (w/v) dried nonfat milk (Carnation)] for 1 h at room temperature. This was removed and replaced with 100 μl of antibody buffer containing 0.1–0.15 μg/ml TG-3 monoclonal antibody (15, 16). This antibody recognizes a phosphoepitope on nucleolin that is present only at mitosis and was provided by Dr. Peter Davies (Albert Einstein College of Medicine, Bronx, NY). After 16–20 h incubation at 4°C, the antibody solution was removed, and the wells were rinsed twice with 200 μl of 10 mM Tris-HCl (pH 7.4), 0.02% Tween 20. HRP-conjugated goat antimouse IgM secondary antibody (Southern Biotechnology Associates) was added at a dilution of 1:500. After overnight incubation at 4°C, the antibody solution was removed, and the wells were rinsed three times with 200 μl of 10 mM Tris-HCl (pH 7.4), 0.02% Tween 20. One hundred μl of 120 mM Na_2HPO_4, 100 mM citric acid (pH 4.0) containing 0.5 μg/ml 2,2'-azino-bis(3-ethylbenzthiazoline-6-sulfonic acid) and 0.01% hydrogen peroxide was added for 1 h at room temperature, and absorbance at 405 nm was determined using a Dynex MRX plate reader.

ELICA of Mitotic Cells. After incubation with extracts, the medium was withdrawn carefully using a pipettor, and 100 μl of 10 mM Tris-HCl (pH 7.4), 150 mM NaCl, containing 3.7% formaldehyde, were added to fix the cells for 30 min at 4°C. The fixative was removed and replaced with 100 μl of cold (−20°C) methanol for 5 min to permeabilize the fixed cells. The methanol was removed, and the wells were rinsed briefly with 200 μl of antibody buffer. Then, 100 μl of antibody buffer containing 0.1–0.15 μg/ml TG-3 monoclonal antibody and HRP-conjugated goat antimouse IgM secondary antibody at a dilution of 1:500 was added for 16–20 h at 4°C. The plates were washed twice with 200 μl of 10 mM Tris-HCl (pH 7.4), 0.02% Tween 20. One hundred μl of 120 mM Na_2HPO_4, 100 mM citric acid (pH 4.0) containing 0.5 μg/ml 2,2'-azino-bis(3-ethylbenzthiazoline-6-sulfonic acid) and 0.01% hydrogen peroxide were added for 1 h at room temperature, and absorbance at 405 nm was measured. Additional information about this assay is provided in "Results."

Sample Collection and Extract Preparation. Approximately 250 g each of marine invertebrates were collected by hand, using scuba, from the cold temperate waters of the Pacific Ocean along the coast of British Columbia, from tropical Pacific Ocean reefs off Motupore and Madang in Papua New Guinea, and from tropical waters off the island of Dominica in the Caribbean. Samples were deep frozen on site and transported to Vancouver over dry ice. Voucher samples of each invertebrate are stored in methanol at −20°C at the University of British Columbia for taxonomic identification. Marine microorganisms were isolated from the invertebrates on site using various marine culture media, and pure cultures were grown as lawns on solid agar marine media in 10-cm Petri plates for several days and then freeze-dried.

Extracts of invertebrates were prepared by homogenizing in methanol ~200 g of each sample. The homogenates were filtered and concentrated to dryness in vacuo to give a gummy residue. Extracts of microorganisms were prepared by extracting the freeze-dried culture (cells and agar) multiple times with dry methanol:acetone, followed by lyophilization. A small amount of each extract was dissolved in DMSO for the antimitotic screen. Extracts of terrestrial plants were obtained from the Open Repository Program of the Natural Products Repository of the NCI Developmental Therapeutics Program as 500-μg samples that were dissolved in 100 μl of DMSO. All diluted extracts were stored at −20°C.

RESULTS

Screen for Antimitotic Agents. The TG-3 monoclonal antibody, originally described as a marker of Alzheimer's disease (15), is highly specific for mitotic cells. Flow cytometry shows that TG-3 immunofluorescence is >50-fold more intense in mitotic cells than in interphase cells (16). In Western blots, the antibody reacts with a M_r 105,000 protein that is present in abundance in extracts of cells treated for 20 h with the antimitotic agent nocodazole but present at only low levels in extracts from cycling MCF-7 cells (Fig. 1). This protein has been identified as a mitotically phosphorylated form of nucleolin (17). Densitometric scanning of the bands showed a 27-fold difference in
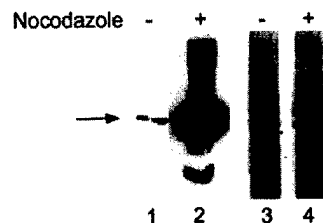

Fig. 1. Western blot, using the TG-3 antibody, of total protein extracts from cycling cells and nocodazole-treated cells (Lanes 1 and 2). Arrow, mitotically phosphorylated form of nucleolin at M_r 105,000. The film was overexposed to illustrate the quantitative difference between cells treated or not with the antimitotic agent. Coomassie blue-stained lanes used as gel loading controls (Lanes 3 and 4).

intensity between nocodazole-treated and untreated cells, corresponding well to the difference in the number of mitotic cells in the two samples: 80% for the nocodazole-treated sample and 3% for the untreated sample, as measured by microscopy.

TG-3 also recognizes mitotic cells in ELISA using microtiter plates (18). In this standard assay (19), cells grown in 96-well plates are lysed, and the lysates are transferred to protein-binding ELISA plates for adsorption to the plastic surface. The antigen is detected by incubating with TG-3 antibody, followed by an HRP-conjugated secondary antibody and colorimetric determination of HRP activity.

We first tested the suitability of the ELISA for quantifying the activity of antimitotic agents. MCF-7 cells were incubated for 20 h with different concentrations of the antimitotic drug paclitaxel, and the proportion of cells arrested in mitosis was measured by counting mitotic figures in the microscope and by ELISA. Paclitaxel induced mitotic arrest in a concentration-dependent manner with half-maximal activity at 10 nM measured by microscopy (Fig. 2A) and at 4 nM measured by ELISA (Fig. 2B).

ELISA is a lengthy and labor-intensive procedure requiring the preparation of cell lysates, their transfer to protein-binding plates, and many solution changes. We subsequently simplified it, reducing the time of the procedure and the number of steps by half and avoiding transfer of samples to ELISA plates. In this procedure, the cells are fixed with formaldehyde in their microtiter culture plate and permeabilized with methanol and detergents, and the TG-3 primary antibody and HRP-conjugated secondary antibody are added simultaneously. Colorimetric detection of HRP activity remains unchanged. Because cell fixation and permeabilization in situ are steps commonly used in immunocytochemistry, we termed the assay ELICA.

The ELICA was tested as above. Dose-dependent arrest of cells in mitosis by paclitaxel was detected by ELICA with half-maximal activity at 1.5 nM (Fig. 2). The ELICA showed a higher signal at low paclitaxel concentrations and a lower signal at high concentrations than did the ELISA (Fig. 2B). These differences probably resulted from higher nonspecific staining of interphase cells because of reduced washing and from lower specific staining of mitotic cells because of fixation and reduced antibody incubation times. Nevertheless, the ELICA consistently showed sufficient difference in absorbance between cells treated or not with antimitotic agents to allow unambiguous detection of mitotic cells. Measurements obtained by ELICA consistently showed smaller SDs than obtained by ELISA, probably because the reduced number of manipulations reduced experimental variation.

Screening of Natural Extracts. We first tested the suitability of the ELISA for drug screening using a small selection of crude extracts from marine microorganisms (Table 1). Of the 264 extracts tested, 261 showed no activity, giving absorbance readings not statistically different from those of untreated cells. Three extracts clearly showed
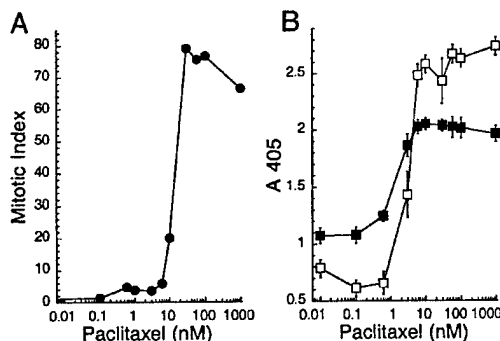
5053

Fig. 2. Evaluation of the ELISA and ELICA using paclitaxel. *A* and *B*, cells were treated with different concentrations of paclitaxel for 20 h, and antimitotic activity was determined using mitotic spreads (●), ELISA (□), or ELICA (■). Experiments were carried out in triplicate, and values indicate means; bars, SD.

activity, with absorbance readings of 1.135, 1.437, and 1.245, close to the values obtained with nocodazole as a positive control.

We then screened over 2000 crude extracts of marine sponges, tunicates, soft corals, starfish, and nudibranchs. This screen identified 16 additional extracts with antimitotic activity. The positive extracts were retested by counting mitotic cells in the microscope, and all were confirmed to arrest cells in mitosis.

Finally, we screened crude extracts of terrestrial plants from the NCI Natural Products Repository by ELICA. The suitability of the ELICA for drug screening is illustrated in Table 2, which displays a screen of 264 plant extracts from three randomly selected 96-well plates. Five extracts showed activity, with absorbance readings close to or higher than those obtained with nocodazole. These positive readings were well above those obtained with negative controls or extracts showing no activity. Of 21,600 plant extracts tested in this manner, 100 showed activity, all of which were confirmed to be positive by microscopy.

All positive extracts from marine organisms and most positive extracts from plants were then rescreened using tubulin immunofluorescence microscopy (14) to examine their effects on microtubule structure. We then purified and identified the active agents in the three microbial extracts, in the single marine invertebrate extract that produced paclitaxel-like bundling of microtubules, and in the terrestrial

plant extract that showed clearest evidence of microtubule bundling. The other extracts remain to be studied.

Identification of New Rhizoxin Analogues. Marine bacterial isolate MK7020 collected off the coast of British Columbia was identified as a *Pseudomonas* sp. by gas chromatographic analysis of cellular fatty acids. The active compounds **1** and **2** (Fig. 3) were purified by chromatographic procedures using the ELISA to guide fractionation. The two other microbial extracts were found to be independent isolates of the same *Pseudomonas* species and contained the same active compounds as MK7020.

Compound **1** is identical to WF-1360C (20, 21), a previously reported analogue of the antimitotic agent rhizoxin (Fig. 3). Compound **1** showed half-maximal antimitotic activity (IC_{50}) at 52 nM, as determined by ELISA (data not shown). Compound **2** is a new δ-lactone seco-hydroxy acid and had an IC_{50} of 8 nM (data not shown).

Identification of New Eleutherobin Analogues. An extract of octocoral *Erythropodium cf. caribaeorum* collected from shallow reefs near Dominica showed antimitotic activity and bundling of microtubules. The active compounds **3–10** (Fig. 4) were isolated, and their chemical structure was elucidated as described in detail elsewhere (22).

Compound **3** was identified as eleutherobin, a recently discovered antimitotic agent that acts like paclitaxel by stabilizing microtubules (23, 24). Compound **4** was identified as sarcodictyin A (25) and differs from eleutherobin by replacement of the C-15 β-linked 2'-O-acetyl-D-arabinopyranose side chain of **3** with a methyl ester and replacement of the C-4 methoxyl with a hydroxyl group. Compounds **5–10** have not been reported previously. Desacetyleleutherobin (**5**) retains the arabinose, but not the 2' acetyl substituent. Isoeleutherobin A (**6**) has an acetyl group at the 3' position instead of the 2' position. Z-Eleutherobin (**7**) is a geometric isomer of eleutherobin at the C-2' to C-3' double bond of the C-8 *N*-(6')-methylurocanic acid ester side chain. Desmethyleleutherobin (**8**) differs from eleutherobin by the presence of a hydroxyl instead of a methoxyl at C-4. Caribaeoside (**9**) differs from eleutherobin by the presence of a hydroxyl at C-11 of the tricyclic core, and a double bond at C-12 to C-13 instead of C-11 to C-12, significantly altering the cyclohexene ring. Caribaeolin (**10**) differs from caribaeoside only by the presence of a –CH_2OCO-CH_3 substituent in the C-3 side chain.

The antimitotic activity profile of these compounds determined by

Table 1 *Pilot ELISA screen of microbial extracts*

96-well plate	A_{405}[a]			
	Positive extracts	Negative extracts	Negative control (no extract added)	Positive control (nocodazole)
A	1.135	0.270 ± 0.051 (n = 86)	0.294 ± 0.098 (n = 4)	1.615 ± 0.068 (n = 4)
	1.437			
B	—	0.280 ± 0.040 (n = 88)	0.267 ± 0.033 (n = 4)	1.298 ± 0.136 (n = 4)
C	1.245	0.276 ± 0.040 (n = 87)	0.305 ± 0.035 (n = 4)	1.448 ± 0.059 (n = 4)

[a] Values shown are mean and SD of the number of measurements shown in parentheses. The absorbance readings are raw data, not corrected for background caused by the microtiter plate and reagents.

Table 2 *ELICA screen of plant extracts*

96-well plate	A_{405}[a]			
	Positive extracts	Negative extracts	Negative control (no extract added)	Positive control (nocodazole)
97040140	2.141	0.731 ± 0.346 (n = 85)	0.752 ± 0.047 (n = 4)	2.379 ± 0.057 (n = 4)
	2.366			
	2.181			
97040141	2.313	0.651 ± 0.198 (n = 88)	0.712 ± 0.048 (n = 4)	1.555 ± 0.113 (n = 4)
97040143	1.421	0.558 ± 0.240 (n = 86)	0.558 ± 0.046 (n = 4)	1.681 ± 0.030 (n = 4)

[a] Values shown are mean and SD of the number of measurements shown in parentheses. The absorbance readings are raw data, not corrected for background caused by the microtiter plate and reagents.
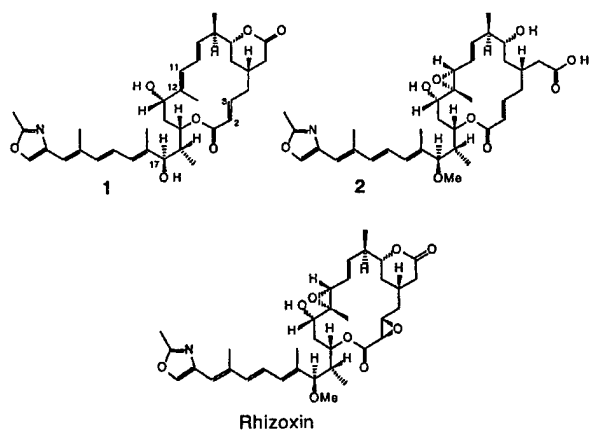
Rhizoxin

Fig. 3. Structural formulae of rhizoxin and analogues.

pilot screen contained members of the rhizoxin family, one marine invertebrate extract contained compounds related to eleutherobin, and a tree extract contained paclitaxel analogues.

Structure-Antimitotic Activity Relationships. The assay is useful not only for identifying and purifying antimitotics but also for providing a quantitative measure of their antimitotic activity. This is a helpful indicator of a compound's pharmacological potential because it measures not simply the interaction of the compound with its target, as an *in vitro* assay would do, but its ability to interact with its target within a cell. We used it to compare the antimitotic activity of different analogues of rhizoxin, eleutherobin, and paclitaxel.

Rhizoxin is a 16-membered macrolide isolated in 1984 (29) and later found to cause the accumulation of cells in mitosis (30, 31) and to inhibit microtubule assembly (31, 32). Rhizoxin is very cytotoxic to cancer cells *in vitro* or in mice (20, 30), including cell lines resistant to the *Vinca* alkaloids (30). It has been the subject of several Phase I and II clinical trials, but results have been disappointing (reviewed in Ref. 33). To the best of our knowledge, the seco-hydroxy acid 2 was not known previously as a natural product, having been reported in the patent literature only as a semisynthetic derivative of the correspond-
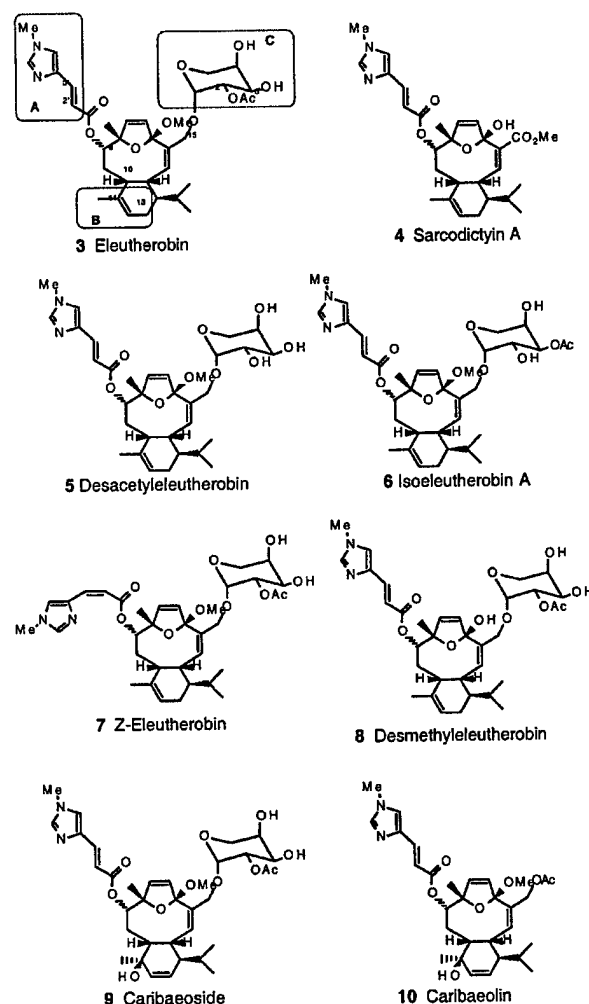
ELICA is shown in Fig. 5. Eleutherobin (3) had an IC_{50} of 100 nM. The activity of Z-eleutherobin (7) was close, with an IC_{50} of 250 nM. Desmethyleleutherobin (8) and isoeleutherobin A (6) were slightly more potent than eleutherobin, with IC_{50} of 20 and 50 nM, respectively. Desacetyleleutherobin (5) was slightly less potent, with an IC_{50} of 400 nM. Sarcodictyin A (4) showed lower activity, with an IC_{50} of 2 μM. Caribaeoside (9) and caribaeolin (10) were considerably less potent, with an IC_{50} of 20 μM for both compounds.

Identification of Paclitaxel Analogues in a Non-*Taxus* Species. NCI Natural Products Repository extract N29701 was obtained from the stem bark of the tree *Ilex macrophylla* in Kalimantan, Indonesia. It showed antimitotic activity and caused bundling of microtubules. The active compounds were isolated and analyzed using ELICA and identified as the known paclitaxel analogues 10-deacetylaxuyunnanine A (11) and 7- (β-xylosyl)-10-deacetyltaxol C (12) (Fig. 6) by analysis of their nuclear magnetic resonance data and comparison with published values (26, 27). Compounds 11 (IC_{50}, 0.3 μM) and 12 (IC_{50}, 10 μM) were much less potent than paclitaxel (IC_{50}, 1.5 nM).

DISCUSSION

Cell-based Assay. We have described a cell-based assay for antimitotic compounds. When searching for therapeutic agents, cell-based assays are particularly valuable compared with cell-free assays because they select not only for activity against a particular target but also for other desirable properties, such as the ability to permeate cells and to retain activity in tissue culture medium and in cells. In one study, >90% of compounds found on the basis of *in vitro* target-based assays showed no cytotoxic activity because they did not cross the plasma membrane or were degraded rapidly (28). In addition, assays based on measuring arrest of cells in mitosis have the potential to identify not only agents that interact with microtubules but also agents that cause mitotic arrest by other mechanisms, such as protein phosphatase inhibitors and mitotic kinesin inhibitors (9-11).

The ELISA and the ELICA procedures both allow unambiguous detection of antimitotic activity in crude natural extracts. The ELICA was used for most of the screening described here because it is faster, less labor-intensive, and less costly than the ELISA.

Our screen of over 24,000 crude extracts from different natural sources identified unambiguously 119 with antimitotic activity. The absence of false-positive results was confirmed by microscopy, and all five positive crude extracts that were subjected to further study yielded known or novel antimitotic agents; three extracts from the

Fig. 4. Structural formulae of eleutherobin and analogues. The *boxed regions A, B,* and *C* of eleutherobin are those considered important for activity in the pharmacophore proposed in (44).

3 Eleutherobin

4 Sarcodictyin A

5 Desacetyleleutherobin

6 Isoeleutherobin A

7 Z-Eleutherobin

8 Desmethyleleutherobin
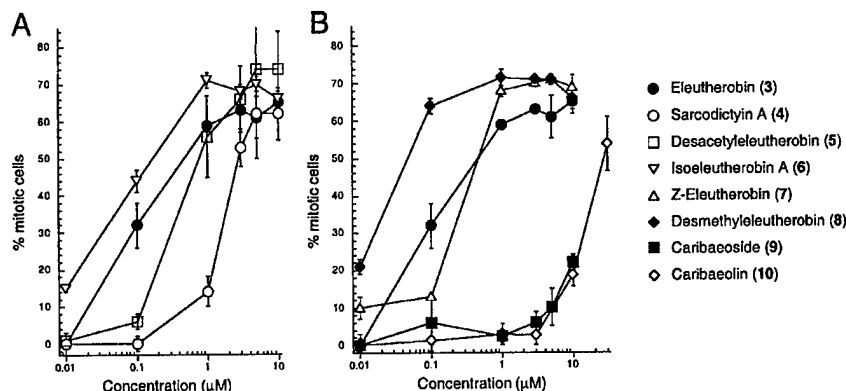
9 Caribaeoside

10 Caribaeolin

Fig. 5. Antimitotic activity of eleutherobin and analogues. Cells were treated with different concentrations of the compounds for 20 h, and mitotic arrest was determined by ELICA. The absorbance values were transformed into the percentage of mitotic cells using a standard curve constructed by measuring the absorbance values of cell populations containing defined percentages of mitotic cells (18). *Bars,* SD.

ing δ-lactone. WF-1360C (1) was 15-fold less toxic to P388 cells than rhizoxin (20). It differs from rhizoxin by the presence of a hydroxyl group instead of a methoxyl at C-17 and the absence of the two epoxides at C-2 to C-3 and C-11 to C-12. Compound 2 retains the methoxyl and one epoxide but has an open lactone ring. Comparison of the antimitotic activity of WF-1360C (IC_{50}, 52 nM) to that of compound 2 (IC_{50}, 8 nM) and to published cytotoxicity data for other analogues (20, 32) indicates that a closed lactone ring is not required for antimitotic activity and that the presence of a methoxyl substituent at C-17 contributes to the high potency of rhizoxin.

Eleutherobin was identified as a compound with paclitaxel-like properties in 1997 (23), but sarcodictyins A-D were the first members of the eleutherobin class of compounds to be identified (25, 34), their paclitaxel-like properties were recognized only later (35). Sarcodictyin A (4) was 20-fold less active than eleutherobin (3), indicating that the C-15 β-linked 2'-O-acetyl-D-arabinopyranose side chain or the C-4 methoxyl group is important for antimitotic activity. Desmethyl-eleutherobin (8) was active, showing that it is the C-15 side chain and not the C-4 methoxyl that is required. Desacetyleleutherobin (5) and isoeleutherobin A (6) showed activity similar to eleutherobin, indicating that the acetyl group does not contribute importantly to activity. Therefore, although the sugar moiety is not absolutely required for antimitotic activity, it contributes to the high potency of eleutherobin.

Isomerization of the C-2' to C-3' double bond of the C-8 side chain of Z-eleutherobin (7) had little effect on the antimitotic activity of the compound, showing that the E configuration in eleutherobin is not required for antimitotic activity. Desmethyleleutherobin (8) was the most active of the compounds tested, suggesting that the C-4 hydroxyl might enhance activity through additional hydrogen bonding, or that the C-4 methoxyl somehow hinders the activity of eleutherobin. Caribaeoside (9) was 200-fold less active than eleutherobin, revealing the importance of the C-11 to C-13 segment for antimitotic activity. Caribaeolin (10) differs from caribaeoside (9) only in the C-3 side chain, and the activities of these compounds are similar. Likewise, sarcodictyin A differs from desmethyleleutherobin only in the C-3 side chain, but its activity is lower than that of desmethyleleutherobin. These data indicate that the C-15 acetyl-D-arabinopyranose can be replaced with an acetoxy functionality without significant loss of activity, confirming earlier data with synthetic analogues (36, 37), but not with a methyl ester.

Thirteen synthetic eleutherobin analogues have recently been described and tested in tubulin polymerization and cytotoxicity assays (36–38). Overall, these studies underlined the importance of the C-8 and C-3 side chains for activity, the C-8 side chain being essential and the sugar or another bulky substituent being needed at C-3 for optimal activity. All of the synthetic analogues retained the original eleuther-

obin core and therefore provided no information about the importance of segments of the tricyclic core.

Eleutherobin represents one of five chemical structural types known to arrest cells in mitosis by stabilizing microtubules. The other four are paclitaxel, discodermolide, the epothilones, and the laulimalides (39–41). Several pharmacophores have been proposed for members of this group (42–44). The latter (44) included eleutherobin and proposed three regions of common overlap between the chemotypes, shown as boxes A, B and C in Fig. 4. Region A of eleutherobin consists of the C-8 side chain, region B encompasses the C-11 to C-13 segment of the tricyclic skeleton, and region C consists of the C-15 substituent. The importance of regions A and C is supported by the published structure-activity data for eleutherobin analogues mentioned above (36–38). Our demonstration that caribaeoside (9), which differs from eleutherobin only in region B, shows a 200-fold lower

11
10-Deacetyltaxuyunnanine A

12
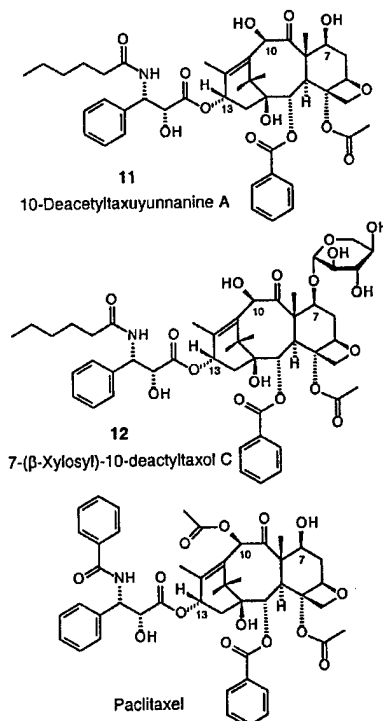7-(β-Xylosyl)-10-deactyltaxol C

Paclitaxel

Fig. 6. Structural formulae of paclitaxel and analogues.

activity demonstrates an important role for this region in antimitotic activity. Further studies will be required to determine whether the reduced antimitotic activity of caribaeoside is attributable to reduced affinity for tubulin and microtubules or to factors such as drug uptake, extrusion, or metabolism.

Paclitaxel is an approved drug for the treatment of advanced ovarian cancer and metastatic breast cancer. It was originally isolated from *Taxus brevifolia* in 1971 (45). Since then, over 350 related diterpenoids have been isolated from different species of the genus *Taxus* (46), including compounds **11** and **12** described here. Compound **11** differs from paclitaxel in the nature of the *N*-acyl substituent on the C-13 phenylisoserine side chain and in the absence of the acetyl substituent at C-10. It was less active than paclitaxel, showing that the C-13 and C-10 substituents, although not essential for activity, contribute to the high potency of paclitaxel. Compound **12** further differs from paclitaxel by the presence of a β-xylosyl substituent at C-7. Compound **12** was less active than compound **11**, indicating that the C-7 substituent also contributes to the potency of paclitaxel.

Unexpected Outcomes. An unexpected outcome of this study is that although the active compounds we isolated belong to known antimitotic chemotypes, they were found in organisms not known or suspected to produce them. To our knowledge, rhizoxin compounds have previously only been isolated from the rice seedling blight fungus *Rhizopus chinensis* and unidentified species of the same genus (29). We have now identified rhizoxin analogues in marine bacterial isolates of the genus *Pseudomonas*, which is common in Pacific Northwest waters. Eleutherobin was originally isolated from the soft coral *Eleutherobia* sp. (possibly *E. albiflora*) collected in Western Australia (23). We now identify eleutherobin in the Caribbean octocoral *Erythropodium caribaeorum*. This is of practical significance because it has not been possible to obtain sufficient amounts of natural or synthetic eleutherobin for preclinical development (47). The taxonomic classification of this source was confirmed by the identification of large quantities of the erythrolide diterpenoids characteristic of this species (48). In contrast to *Eleutherobia*, *E. caribaeorum* is widespread in the Caribbean and Florida (49–51), abundant in certain areas, and has been grown in aquaria. It may thus constitute a suitable source of eleutherobin for preclinical and early phase clinical trials. Paclitaxel and analogues have all been isolated from the bark of yew trees (46), from endophytic fungi isolated from the *Taxus* species or *Taxodium distichum* (52, 53), and recently from an epiphytic fungus on the rubiaceous plant *Maguireothamnus speciosus* (54). It was surprising to find paclitaxel analogues in the bark of a non-*Taxus* tree. The taxonomic classification of our extract was confirmed by the presence of the triterpenoid glycosides characteristic of the genus *Ilex* (55). It is possible that an endophytic fungus is responsible for their production in *Ilex macrophylla*.

Perhaps the most important outcome of this study is that the assay permitted us to detect antimitotic agents in extracts that were not found to contain them using other methods. *E. caribaeorum* has been subjected to extensive chemical characterization (48), but eleutherobin compounds were not detected because they are very minor components. The COMPARE algorithm, which is able to detect similar differential patterns of growth inhibition for the 60 human cell lines in the NCI anticancer drug screen, has been used successfully to identify new antimitotic agents within the NCI chemical repository of pure compounds (13). Extracts in the NCI Natural Products Repository have also been tested against the NCI cell line panel. A COMPARE analysis using paclitaxel as the probe compound identified 47 plant extracts with a Pearson correlation coefficient above 0.6 (not shown). Three of these extracts were positive in our antimitotic screen, and all three were from *Catharanthus roseus*, the plant from which the *Vinca* alkaloids were originally isolated (1). The analysis

did not identify the extract from *Ilex macrophylla*, the growth inhibition pattern of which does not resemble that of paclitaxel and other antimitotic compounds. This illustrates the usefulness of the cell-based assay for the identification of active compounds present in very low abundance in crude natural extracts. The assay should greatly facilitate the discovery and development of novel antimitotic agents and their characterization in the context of living cells.

REFERENCES

1. Rowinsky, E. K., and Donehower, R. C. Antimicrotubule agents. *In:* B. A. Chabner and D. L. Longo (eds.), Cancer Chemotherapy and Biotherapy, pp. 263–296. Philadelphia: Lippincott-Raven Publishers, 1996.
2. Rowinsky, E. K. The development and clinical utility of the taxane class of antimicrotubule chemotherapy agents. Annu. Rev. Med., *48:* 353–374, 1997.
3. Jordan, M. A., Thrower, D., and Wilson, L. Effects of vinblastine, podophyllotoxin, and nocodazole on mitotic spindles. Implications for the role of microtubule dynamics in mitosis. J. Cell Sci., *102:* 401–416, 1992.
4. Jordan, M. A., Toso, R. J., Thrower, D., and Wilson, L. Mechanism of mitotic block and inhibition of cell proliferation by Taxol at low concentrations. Proc. Natl. Acad. Sci. USA, *90:* 9552–9556, 1993.
5. Jordan, M. A., and Wilson, L. Microtubules and actin filaments: dynamic targets for cancer chemotherapy. Curr. Opin. Cell Biol., *10:* 123–130, 1998.
6. Torres, K., and Horwitz, S. B. Mechanisms of Taxol-induced cell death are concentration-dependent. Cancer Res., *58:* 3620–3626, 1998.
7. Panda, D., Miller, H. P., Islam, K., and Wilson, L. Stabilization of microtubule dynamics by estramustine by binding to a novel site in tubulin: a possible mechanistic basis for its antitumor action. Proc. Natl. Acad. Sci. USA, *94:* 10560–10564, 1997.
8. Hudes, G. Estramustine-based chemotherapy. Semin. Urol. Oncol., *15:* 13–19, 1997.
9. Roberge, M., Tudan, C., Hung, S. M., Harder, K. W., Jirik, F. R., and Anderson, H. Antitumor drug fostriecin inhibits the mitotic entry checkpoint and protein phosphatases 1 and 2A. Cancer Res., *54:* 6115–6121, 1994.
10. Cheng, A., Balczon, R., Zuo, Z., Koons, J. S., Walsh, A. H., and Honkanen, R. E. Fostriecin-mediated G2-M-phase growth arrest correlates with abnormal centrosome replication, the formation of aberrant mitotic spindles, and the inhibition of serine/threonine protein phosphatase activity. Cancer Res., *58:* 3611–3619, 1998.
11. Mayer, T. U., Kapoor, T. M., Haggarty, S. J., King, R. W., Schreiber, S. L., and Mitchison, T. J. Small molecule inhibitor of mitotic spindle bipolarity identified in a phenotype-based screen. Science (Washington DC), *286:* 971–974, 1999.
12. Jordan, A., Hadfield, J. A., Lawrence, N., J., and McGown, A. T. Tubulin as a target for anticancer drugs: agents which interact with the mitotic spindle. Med. Res. Rev., *18:* 259–296, 1998.
13. Paull, K. D., Lin, C. M., Malspeis, L., and Hamel, E. Identification of novel antimitotic agents acting at the tubulin level by computer-assisted evaluation of differential cytotoxicity data. Cancer Res., *52:* 3892–3900, 1992.
14. Anderson, H. J., Coleman, J. E., Andersen, R. J., and Roberge, M. Cytotoxic peptides hemiasterlin, hemiasterlin A and hemiasterlin B induce mitotic arrest and abnormal spindle formation. Cancer Chemother. Pharmacol., *39:* 223–226, 1997.
15. Vincent, I., Rosado, M., and Davies, P. Mitotic mechanisms in Alzheimer's disease? J. Cell Biol., *132:* 413–425, 1996.
16. Anderson, H. J., deJong, G., Vincent, I., and Roberge, M. Flow cytometry of mitotic cells. Exp. Cell Res., *238:* 498–502, 1998.
17. Dranovsky, A., Gregori, L., Schwartzman, A., Vincent, I., Davies, P., and Goldgaber, D. Distribution of nucleolin in Alzheimer's disease and control brains. Soc. Neurosci. Abstracts, *27:* 2219, 1997.
18. Roberge, M., Berlinck, R. G. S., Xu, L., Anderson, H. J., Lim, L. Y., Curman, D., Stringer, C. M., Friend, S. H., Davies, P., Haggarty, S. J., Kelly, M. T., Britton, R., Piers, E., and Andersen, R. J. High-throughput assay for G2 checkpoint inhibitors and identification of the structurally novel compound isogranulatimide. Cancer Res., *58:* 5701–5706, 1998.
19. Perlmann, H., and Perlmann, P. Enzyme-linked immunosorbent assay. *In:* J. E. Celis (ed.) Cell Biology–A practical Approach, Vol. 2, pp. 322–328. San Diego: Academic Press, 1994.
20. Kiyoto, S., Kawai, Y., Kawakita, T., Kino, E., Okuhara, M., Uchida, I., H., T., Hashimotot, M., Terano, H., Kohsaka, M., Aoki, H., and Imanaka, H. A new antitumor complex, WF-1360, WF-1360A, B, C, D, E, and F. J. Antibiot. (Tokyo), *39:* 762–772, 1986.
21. Iwasaki, S., Namikoshi, M., Kobayashi, H., Furukawa, J., and Okuda, S. Studies on macrocyclic antibiotics. IX. Novel macrolides from the fungus *Rhizopus chinensis:* precursors of rhizoxin. Chem. Pharm. Bull., *34:* 1387–1390, 1986.
22. Cinel, B., Roberge, M., Behrisch, H., van Ofwegen, L., Castro, C. B., and Andersen, R. J. Antimitotic diterpenes from *Erythropodium caribaeorum* test pharmacophore models for microtubule stabilization. Org. Lett., *2:* 257–260, 2000.

23. Lindel, T., Jensen, P. R., Fenical, W., Long, B. H., Casazza, A. M., Carboni, J., and Fairchild, C. R. Eleutherobin, a new cytotoxin that mimics paclitaxel (Taxol) by stabilizing microtubules. J. Am. Chem. Soc., *119:* 8744–8745, 1997.

24. Long, B. H., Carboni, J. M., Wasserman, A. J., Cornell, L. A., Casazza, A. M., Jensen, P. R., Lindel, T., Fenical, W., and Fairchild, C. R. Eleutherobin, a novel cytotoxic agent that induces tubulin polymerization, is similar to paclitaxel (Taxol). Cancer Res., *58:* 1111–1115, 1998.

25. D'Ambrosio, M., Guerriero, A., and Pietra, F. Sarcodictyin A and Sarcodictyin B, novel deiterpenoidic alcohols esterified by (E)-N(1)-methylurocanic acid. Isolation from the Mediterranean stolonifer *Sarcodictyon roseum.* Helv. Chim. Acta, *70:* 2019–2027, 1987.

26. Morita, H., Gonda, A., Wei, L., Yamamura, Y., Wakabayashi, H., Takeya, K., and Itokawa, H. Four new taxoids from *Taxus cuspidata* var. nana. Planta Med., *64:* 183–186, 1998.

27. Senilh, V., Blechert, S., Colin, M., Guenard, D., Potier, F. P., and Varenne, P. Mise en evidence de nouveaux analogues du Taxol extraits de *Taxus baccata.* J. Nat. Prod., *47:* 131–137, 1984.

28. Corbett, T., Valeriote, F., LoRusso, P., Polin, L., Panchapor, C., Pugh, S., White, K., Knight, J., Demchik, L., Jones, J., Jones, L., and Lisow, L. *In vivo* methods for screening and preclinical testing. *In:* B. Teicher (ed.), Drug Development Guide, pp. 75–99. Totowa, NJ: Humana Press, Inc., 1997.

29. Iwasaki, S., Kobayashi, H., Furukawa, J., Namikoshi, M., Okuda, S., Sato, Z., Matsuda, I., and Noda, T. Studies on macrocyclic lactone antibiotics. VIII. Structure of a phytotoxin "rhizoxin" produced by *Rhizopus chinensis.* J. Antibiot., *37:* 354–362, 1984.

30. Tsuruo, T., Oh-hara, T., Iida, H., Tsukagoshi, S., Sato, Z., Matsuda, I., Iwasaki, S., Okuda, S., Shimizu, F., Sasagawa, K., Fukami, M., Fukuda, K., and Arakawa, M. Rhizoxin, a macrocyclic lactone antibiotic, as a new antitumor agent against human and murine tumor cells and their vincristine-resistant sublines. Cancer Res., *46:* 381–385, 1986.

31. Bai, R., Pettit, G. R., and Hamel, E. Dolastatin, a powerful cytostatic peptide derived from a marine animal: inhibition of tubulin polymerization mediated through the Vinca alkaloid binding domain. Biochem. Pharmacol., *39:* 1941–1949, 1990.

32. Takahashi, M., Iwasaki, S., Kobayashi, H., and Okuda, S. Studies on macrocyclic lactone antibiotics. XI. Anti-mitotic and anti-tubulin activity of new antitumor antibiotics, rhizoxin and its homologues. J. Antibiot., *40:* 66–72, 1987.

33. Christian, M. C., Pluda, J. M., Ho, P. T. C., Arbuck, S. G., Murgo, A. J., and Sausville, E. A. Promising new agents under development by the division of cancer treatment, diagnosis, and centers of the National Cancer Institute. Semin. Oncol., *24:* 219–240, 1998.

34. D'Ambrosio, M., Guerriero, A., and Pietra, F. Isolation from the Mediterranean stoloniferan coral *Sarcodictyon roseum* of sarcodictyin C, D, E, and F, novel diterpenoidic alcohols esterified by (E)- or (Z)-N(1)-methylurocanic acid. Failure of the carbon-skeleton type as a classification criterion. Helv. Chim. Acta, *71:* 964–976, 1988.

35. Ciomei, M., Albanese, C., Pastori, W., Grandi, M., Pietra, F., D'Ambrosio, M., Guerriero, A., and Battistini, C. Sarcodictyins: a new class of marine derivatives with mode of action similar to Taxol. Proc. Am. Assoc. Cancer Res., *38:* 5, 1997.

36. Nicolaou, K. C., Kim, S., Pfefferkorn, J., Xu, J., Ohshima, T., Hosokawa, S., Vourloumis, D., and Li, T. Synthesis and biological activity of sarcodictyins. Angew. Chem. Int. Ed. Engl., *37:* 1418–1421, 1998.

37. McDaid, H. M., Bhattacharya, S. K., Chen, X-T., He, L., Shen, H-J., Gutteridge, C. E., Horwitz, S. B., and Danishefsky, S. J. Structure-activity profiles of eleutherobin analogs and their cross-resistance in Taxol-resistant cell lines. Cancer Chemother. Pharmacol., *44:* 131–137, 1999.

38. Hamel, E., Sackett, D. L., Vourloumis, D., and Nicolaou, K. C. The coral-derived natural products eleutherobin and sarcodictyins A and B: effects on the assembly of purified tubulin with and without microtubule-associated proteins and binding at the polymer taxoid site. Biochemistry, *38:* 5490–5498, 1999.

39. ter Haar, E., Kowalski, R. J., Hamel, E., Lin, C. M., Longley, R. E., Gunasekara, S. P., Rosenkranz, H. S., and Day, B. W. Discodermolide, a cytotoxic marine agent that stabilizes microtubules more potently than Taxol. Biochemistry, *35:* 243–250, 1996.

40. Bollag, D. M., McQueney, P. A., Zhu, J., Hensens, O., Koupal, L., Liesch, J., Goetz, M., Lazarides, E., and Woods, C. M. Epothilones, a new class of microtubule-stabilizing agents with a Taxol-like mechanism of action. Cancer Res., *55:* 2325–2333, 1995.

41. Mooberry, S. L., Tien, G., Hernandez, A. H., Plubrukarn, A., and Davidson, B. S. Laulimalide and isolaulimalide, new paclitaxel-like microtubule-stabilizing agents. Cancer Res., *59:* 653–660, 1999.

42. Winkler, J. D., and Axelsen, P. H. A model for the Taxol (paclitaxel)/epothilone pharmacophore. Bioorg. Med. Chem. Lett., *6:* 2963–2966, 1996.

43. Wang, M., Xia, X., Kim, Y., Hwang, D., Jansen, J. M., Botta, M., Liotta, D. C., and Snyder, J. P. A unified and quantitative receptor model for the microtubule binding of paclitaxel and epothilone. Org. Lett., *1:* 43–46, 1999.

44. Ojima, I., Chakravarty, S., Inoue, T., Lin, S., He, L., Band Horwitz, S., Kuduk, S. D., and Danishefsky, S. J. A common pharmacophore for cytotoxic natural products that stabilize microtubules. Proc. Natl. Acad. Sci. USA, *96:* 4256–4261, 1999.

45. Wani, M. C., Taylor, H. L., Wall, M. E., Coggon, P., and McPhail, A. T. Plant antitumor agents. VI. The isolation and structure of Taxol, a novel antileukemic and antitumor agent from *Taxus brevifolia.* J. Am. Chem. Soc., *93:* 2325–2327, 1971.

46. Baloglu, E., and Kingston, D. G. I. The taxane diterpenoids. J. Nat. Prod., *62:* 1448–1472, 1999.

47. Rayl, A. J. S. Oceans: medicine chests of the future? Scientist, *13:* 1–5, 1999.

48. Look, S. A., Fenical, W., Van Engen, D., and Clardy, J. Erythrolides: unique marine diterpenoids interrelated by a naturally occurring di-π-methane rearrangement. J. Am. Chem. Soc., *106:* 5026–5027, 1984.

49. Kinzie, R. A. The zonation of West Indian gorgonians. Bull. Mar. Sci., *23:* 93–115, 1973.

50. Goldberg, W. M. The ecology of the coral-octocoral communities off the Southeast Florida coast: geomorphology, species composition, and zonation. Bull. Mar. Sci., *23:* 465–488, 1973.

51. Opresko, D. M. Abundance and distribution of shallow-water gorgonians in the area of Miami, Florida. Bull. Mar. Sci., *23:* 535–558, 1973.

52. Li, J. Y., Strobel, G., Sidhu, R. H., Hess, W. M., and Ford, E. J. Endophytic Taxol-producing fungi from bald cypress *Taxodium distichum.* Microbiology, *142:* 2223–2226, 1996.

53. Strobel, G., Yang, X., Sears, J., Kramer, R., Sidhu, R. S., and W. M. Hess, Taxol from *Pestalotiopsis microspora,* an endophytic fungus of *Taxus wallachiana.* Microbiology, *142:* 435–440, 1996.

54. Strobel, G. A., Ford, E., Li, J. Y., Sears, J., Sidhu, R. S., and Hess, W. M. *Semiatoantlerium tepuiense* gen. nov., a unique epiphytic fungus producing Taxol from the Venezuelan Guyana. Syst. Appl. Microbiol., *22:* 426–433, 1999.

55. Gosmann, G., Guillame, D., Taketa, A. T. C., and Schenkel, E. P. Triterpenoid saponins from *Ilex paraguariensis.* J. Nat. Prod., *58:* 438–441, 1995.

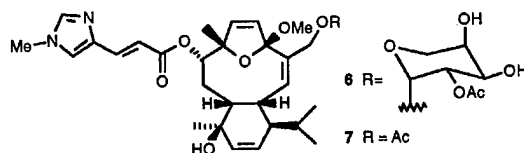# Antimitotic Diterpenes from *Erythropodium caribaeorum* Test Pharmacophore Models for Microtubule Stabilization

Bruno Cinel,[†] Michel Roberge,[‡] Hans Behrisch,[§] Leen van Ofwegen,[‖]
Clovis B. Castro,[⊥] and Raymond J. Andersen[*,†]

*Departments of Chemistry and Oceanography (EOS), University of British Columbia,
Vancouver, B.C., Canada, V6T 1Z1, Department of Biochemistry and Molecular
Biology, University of British Columbia, Vancouver, B.C., Canada, V6T 1Z3, Ross
University Medical School, Commonwealth of Dominica, Nationaal Natuurhistorisch
Museum, Leiden, The Netherlands, and Museu Nacional, Rio de Janeiro, Brazil*

randersn@unixg.ubc.ca

Received October 29, 1999

ABSTRACT

Six new antimitotic diterpenes, 2–7, have been isolated from the Caribbean octocoral *Erythropodium caribaeorum*. Structural variations encountered in this group of natural products test recently proposed pharmacophore models for microtubule stabilizing compounds.

Antimitotic compounds interfere with the dynamic assembly and disassembly of α- and β-tubulin into microtubules, causing cells to arrest in mitosis.[1] Prolonged arrest in mitosis eventually leads to cell death, mainly by apoptosis. Two chemical classes of antimitotic agents, the vinca alkaloids (vinblastine, vincristine, and vinorelbine) and the taxanes (paclitaxel and docetaxel), are clinically useful anticancer drugs. Most known antimitotic agents, including the vinca alkaloids, induce mitotic arrest by inhibiting the polymerization of tubulin into microtubules. Paclitaxel was the first chemical entity shown to cause mitotic arrest by stabilizing

microtubules against depolymerization. Since the initial discovery of paclitaxel's mechanism of action and its introduction into clinical use, there has been much interest in finding other chemical structural types that also stabilize microtubules. Four additional chemotypes that have paclitaxel-like effects have subsequently been identified. These include the myxobacterium metabolites epothilones A and B,[2] the marine sponge metabolites discodermolide,[3] laulimalide, and isolaulimalide,[4] and the soft coral metabolite eleutherobin.[5] Ojima et al. have recently proposed a common pharmacophore for the microtubule stabilizing compounds that effectively accommodates nonataxel, paclitaxel, disco-

† Departments of Chemistry and Oceanography (EOS), University of British Columbia.
‡ Department of Biochemistry and Molecular Biology, University of British Columbia.
§ Ross University Medical School.
‖ Nationaal Natuurhistorisch Museum.
⊥ Museu Nacional.
(1) (a) Jordan, A.; Hadfield, J. A.; Lawrence, N. J.; McGowen, A. T. *Med. Res. Rev.* **1998**, *18*, 259–296. (b) Hamel, E. *Ibid.* **1996**, *16*, 207–231.

(2) Bollag, D. M.; McQueney, P. A.; Zhu, J.; Hensens, O.; Koupal, L.; Liesch, J.; Goetz, M.; Lazarides, E.; Woods, C. M. *Cancer Res.* **1995**, *55*, 2325–2333.
(3) ter Haar, E.; Kowalski, R. J.; Hamel, E.; Lin, C. M.; Longley, R. E.; Gunasekera, S. P.; Rosenkranz, H. S.; Day, B. W. *Biochemistry* **1996**, *35*, 243–250.
(4) Mooberry, S. L.; Tien, G.; Hernandez, A. H.; Plubrukarn, A.; Davidson, B. S. *Cancer Res.* **1999**, *59*, 653–660.

dermolide, eleutherobin, and the epothilones.[6] This model predicts that three regions of eleutherobin (1) (see boxes A, B, and C below) are important domains for binding to tubulin.

1
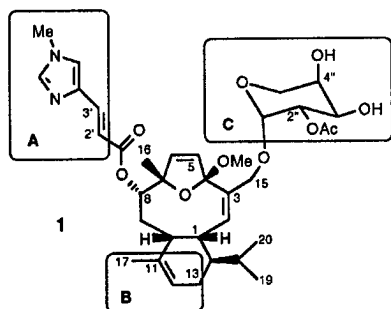
Most known antimitotic natural products were initially isolated because they exhibited potent in vitro cytotoxicity, and only subsequent mechanism of action studies revealed that they interfered with tubulin assembly and disassembly dynamics. Two classes of antimitotic agents, the epothilones[2] and the laulimalides,[4] have been discovered by rational screening, illustrating the significant potential for assay-directed identification of novel antimitotic chemotypes. Recently, a new cell-based antimitotic assay that is rapid and reliable has been developed in one of our laboratories.[7] Extracts of the octocoral *Erythropodium caribaeorum* collected at several sites in the Southern Caribbean showed potent activity in the assay.[8] Microscopic examination of cells arrested in mitosis by the *E. caribaeorum* extract showed evidence of tubulin bundling, similar to the effects of paclitaxel.

Bioassay guided fractionation of the *E. caribaeorum* extract led to the isolation of eleutherobin (1) and the new antimitotic diterpenoids desmethyleleutherobin (2), desacetyleleutherobin (3), isoeleutherobin A (4), Z-eleutherobin (5), caribaeoside (6), and caribaeolin (7). Compounds 3–7 all differ from eleutherobin in the proposed A, B, and C tubulin binding regions. In particular, caribaeoside (6) provides the first test for the B region in Ojima's model of the eleutherobin pharmacophore.

Freshly collected specimens of *E. caribaeorum* were frozen on site and transported to Vancouver over dry ice.

(5) (a) Lindel, T.; Jensen, P. R.; Fenical, W.; Long, B. H.; Casazza, A. M.; Carboni, J.; Fairchild, C. R. *J. Am. Chem. Soc.* **1997**, *119*, 8744–8745. (b) Long, B. H.; Carboni, J. M.; Wasserman, A. J.; Cornell, L. A.; Casazza, A. M.; Jensen, P. R.; Lindel, T.; Fenical, W.; Fairchild, C. R. *Cancer Res.* **1998**, *58*, 1111–1115. (c) Hamel, E.; Sackett, D. L.; Vourloumis, D.; Nicolaou, K. C. *Biochemistry* **1999**, *38*, 5490–5498.

(6) Ojima, I.; Chakravarty, S.; Inoue, T.; Lin, S.; He, L.; Horwitz, S. W.; Kuduk, S. D.; Danishefsky, S. J. *Proc. Natl. Acad. Sci. U.S.A.* **1999**, *96*, 4256–4261.

(7) Roberge, M.; Cinel, B.; Anderson, H.; Lim, L.; Jiang, X.; Xu, L.; Kelly, M. T.; Andersen, R. J. *Cancer Res.* Submitted for publication.

(8) For previous chemical studies of *E. caribaeorum*, see: (a) Maharaj, D.; Pascoe, K. O.; Tinto, W. F. *J. Nat. Prod.* **1999**, *62*, 313–314. (b) Pathirana, C.; Fenical, W. F.; Corcoran, E.; Clardy, J. *Tetrahedron Lett.* **1993**, *34*, 3371–3372. (c) Pordesimo E. O.; Schmitz, F. J.; Ciereszko, L. S.; Hossain, M. B.; Van der Helm, D. *J. Org. Chem.* **1991**, *56*, 2344–2357. (d) Look, S. A.; Fenical, W. F.; Van Engen, D.; Clardy, J. *J. Am. Chem. Soc.* **1984**, *106*, 5026–5027.

Thawed samples (5.3 kg wet wt) were extracted multiple times with MeOH, and the combined MeOH extracts were concentrated to a gum in vacuo. Fractionation of the crude gum (280 g) by sequential application of vacuum reversed-phase flash (gradient elution: 80:20 H$_2$O/MeOH to MeOH in 10% increments), normal-phase flash (gradient elution: EtOAc to 80:20 EtOAc/MeOH in 2% increments), and normal-phase high-performance liquid chromatographies (eluent: 93:7 CH$_2$Cl$_2$/MeOH) gave pure samples of 1 (50 mg), 2 (7 mg), 3 (6 mg), 4 (3 mg), and 5 (2 mg). Compounds 6 (1 mg) and 7 (1 mg) partially decomposed on silica gel so they were isolated using only vacuum reversed-phase flash chromatography and cyano-bonded-phase HPLC (eluent: 56:42:2 EtOAc/hexane/(^{i}Pr)$_2$NH).
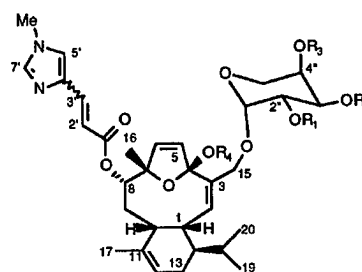
2 R$_1$ = Ac; R$_2$ = R$_3$ = R$_4$ = H; Δ$^{2',3'}$ (E)

3 R$_1$ = R$_2$ = R$_3$ = H; R$_4$ = Me; Δ$^{2',3'}$ (E)

4 R$_1$ = R$_3$ = H; R$_2$ = Ac; R$_4$ = Me; Δ$^{2',3'}$ (E)

5 R$_1$ = Ac; R$_2$ = R$_3$ = H; R$_4$ = Me; Δ$^{2',3'}$ (Z)

8 R$_1$ = R$_2$ = R$_3$ = Ac; R$_4$ = Me; Δ$^{2',3'}$ (E)

All NMR data for the *E. caribaeorum* diterpenes were recorded in DMSO-d_6 at 500 MHz. Tables of the NMR assignments are available in the Supporting Information. Eleutherobin (1) was identified by comparison of its spectroscopic data with literature values.[5a] Desmethyleleutherobin (2) was isolated as a clear oil that gave a [M + H]$^+$ ion in the HRFABMS at *m/z* 643.32230, appropriate for a molecular formula of C$_{34}$H$_{46}$N$_2$O$_{10}$ (ΔM −1.21 ppm), that differed from the molecular formula of eleutherobin simply by the loss of CH$_2$. The ^{1}H NMR spectrum of 2 differed from the ^{1}H NMR spectrum of eleutherobin (1) only by the absence of a methyl resonance at ∼δ 3.1 that could be assigned to the C-4 methoxyl substituent. This evidence indicated that 2 was identical to eleutherobin (1) except for the presence of a hydroxyl group instead of a methoxyl group at C-4. The 2D NMR data obtained for 2 was in complete agreement with this assignment.

Desacetyleleutherobin (3) was isolated as a clear oil that gave a [M + H]$^+$ ion at *m/z* 615.32813 in the HRFABMS corresponding to a molecular formula of C$_{33}$H$_{46}$N$_2$O$_9$ (ΔM −0.05 ppm), which differed from the formula of eleutherobin (1) by the loss of C$_2$H$_2$O. The ^{1}H NMR spectrum of 3 showed a strong resemblence to the ^{1}H NMR spectrum of eleutherobin (1) except for the absence of a methyl singlet at ∼δ 2 that could be assigned to an acetyl residue and the chemical shifts of the resonances assigned to the arabinose protons. These NMR differences suggested that 3 was simply the

desacetyl analogue of eleutherobin (**1**). Acetylation of **3** with acetic anhydride in pyridine converted it to diacetyleleutherobin (**8**), which was identical to **8** prepared by acetylation of eleutherobin using the same reaction conditions, confirming the proposed structure of **3**.

Isoeleutherobin A (**4**), isolated as a clear oil, gave an [M + H]$^+$ ion at *m/z* 657.33834 in the HRFABMS corresponding to a molecular formula of $C_{35}H_{48}N_2O_{10}$ (ΔM −0.58 ppm), which was identical to the molecular formula of eleutherobin (**1**). Comparison of the ^{1}H 1D and 2D NMR data for isoeleutherobin A (**4**) with the data for eleutherobin (**1**) showed that the molecules differed only in the position of acetylation on the arabinose fragment. COSY correlations observed between resonances at δ 3.38 and 3.62 (both broad doublets: *J* = 12.2 Hz), assigned to the C-5″ methylene protons, and a methine at δ 3.83 (H-4″: m) showed that the acetate was not at C-4″. The H-4″ resonance in turn showed a COSY correlation to a resonance at δ 4.80 (dd, *J* = 2.5, 10.1 Hz), assigned to H3″, which was significantly deshielded relative to the corresponding H3″ resonance (δ 3.73) in eleutherobin (**1**). Therefore, isoeleutherobin A was assigned structure **4**. Acetylation with acetic anhydride in pyridine converted isoeleutherobin A (**4**) to diacetyleleutherobin (**8**), confirming the assigned structure of **4**.

Z-Eleutherobin (**5**) gave a [M + H]$^+$ ion at *m/z* 657.33830 in the HRFABMS appropriate for a molecular formula of $C_{35}H_{48}N_2O_{10}$ (ΔM −0.65 ppm), again identical to the molecular formula of eleutherobin (**1**). Comparison of the NMR data obtained for **5** with the data for **1** showed that the molecules differed only in the configuration of the $\Delta^{2',3'}$ olefin. In the ^{1}H NMR spectrum of Z-eleutherobin (**5**), the uroconic acid olefinic proton resonances appeared at δ 5.75 (H-2′) and 6.94 (H-3′) with a coupling constant of 12.6 Hz, whereas in the spectrum of eleutherobin (**1**) they were found at δ 6.35 (H-2′) and 7.53 (H-3′) with a coupling constant of 15.6 Hz. The NMR sample of Z-eleutherobin (**5**) partially isomerized over time to eleutherobin (**1**), confirming the assigned structure.

6 R=

7 R = Ac
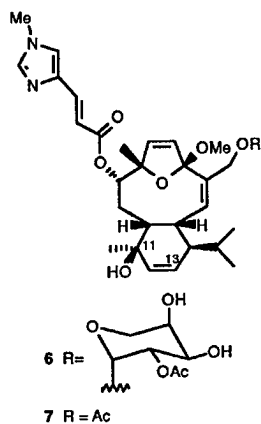
Caribaeoside (**6**), obtained as a colorless glass, gave a [M + H]$^+$ ion in the HRFABMS at *m/z* 673.33474 appropriate for a molecular formula of $C_{35}H_{48}N_2O_{11}$ (ΔM 1.64 ppm),

that only differed from the molecular formula of eleutherobin (**1**) by the presence of one additional oxygen atom. Analysis of the NMR data obtained for caribaeoside (**6**) revealed that it too was a diterpene glycoside with the same *N-(6′)*-methyluroconic acid and 2″-*O*-acetylarabinose substituents that are attached to the central core of eleutherobin (**1**).

A number of features of the NMR data revealed that caribaeoside (**2**) and eleutherobin (**1**) differed in the C-11 to C-13 regions of their diterpene cores. The C-17 olefinic methyl resonance at δ 1.47 and the H-12 olefinic methine resonance at δ 5.27 in the ^{1}H NMR spectrum of eleutherobin (**1**) were both missing in the ^{1}H NMR spectrum of caribaeoside (**6**). In their place, the ^{1}H NMR spectrum of **6** had a singlet methyl resonance at δ 0.82 and a pair olefinic methine resonances at δ 5.52−5.54 (H-12 and H-13). The two-proton olefinic resonance showed correlations in the HMQC spectrum to carbon resonances at δ 125.6 (C-13) and 137.4 (C-12). HMBC correlations observed between the Me-17 singlet at δ 0.82 and the C-12 olefinic resonance at δ 137.4, a quaternary carbon resonance at δ 68.3, and a methine resonance at δ 45.7 (HMQC to δ 2.07) confirmed the proximity of Me-17 and C-12 and indicated that there was a hydroxyl substituent at C-11 and a methine carbon at C-10.[9] A pair of overlapping doublets (6H) at δ 0.94−0.95, that showed COSY correlations to a methine resonance at δ 1.68, were assigned to the Me-19 and Me-20 isopropyl protons, and a multiplet at δ 4.00, that showed COSY correlations to an olefinic doublet at δ 5.38 (H-2) and a methine resonance at δ 2.07 (H-10), was assigned to H-1. The H-1 resonance in the spectrum of **6** had a chemical shift and multiplicity nearly identical to the H-1 resonance in eleutherobin (**1**) (δ 3.88), consistent with the proposal that the C-1, C-2, C-10, and C-14 centers in **6** were identical to the corresponding sites in **1**.

ROESY and scalar coupling constant data established the relative stereochemistry about the cyclohexene ring in caribaeoside (**6**). The resonances assigned to H-1 (δ 4.00) and H-2 (δ 5.38) in **6** had chemical shifts and a vicinal coupling constant (*J* = 9.7 Hz) nearly identical with their counterparts in eleutherobin (**1**) (δ H-1, 3.88; H-2, 5.39: *J* = 9.4 Hz), indicating that the dihedral angle between them in **6** was essentially identical to that in **1**. ROESY correlations observed between the isopropyl methyl proton resonances at δ 0.94−0.95 and the H-1 (δ 4.00) and H-10 (δ 2.07) resonances in **6**, demonstrated that the isopropyl group, H-1, and H-10 were on the same face of the molecule, as in eleutherobin (**1**). The Me-17 resonance at δ 0.82 in **6** showed a strong ROESY correlation to the H-2 (δ 5.38) resonance demonstrating that Me-17 and C-2 were cis. Models indicate that the Me-17 protons can sit in the shielding region of the $\Delta^{2,3}$ olefin, consistent with their unusually shielded chemical shift of δ 0.82. ROESY correlations observed between Me-16 (δ 1.33) and both H-8 (δ 4.85) and OMe-21 (δ 3.08), and between H-8 and H-10 (δ 2.07), confirmed that car-

(9) Sarcodictyin F, a related 4,7-oxaeunicellane diterpenoid, has a similarly functionalized cyclohexene ring, but with the opposite stereochemistry at C-11. See: D'Ambrosio, M.; Guerriero, A.; Pietra, F. *Helv. Chim. Acta* **1988**, *71*, 964−976.

ibaeoside (**6**) and eleutherobin (**1**) had identical relative stereochemistries at C-4, C-7, C-8, and C-10.

Caribaeolin (**7**) was isolated as a clear oil that gave a [M + H]$^+$ ion in the HRFABMS at m/z 541.29111 corresponding to a molecular formula of $C_{30}H_{40}N_2O_7$ (ΔM −0.49 ppm). Analysis of the 1D and 2D ^1H detected NMR data obtained for **7** revealed that it contained the diterpene core and *N-(6′)-*methyluroconic acid fragments that constitute the aglycon of caribaeoside (**6**) but was missing the arabinose sugar residue. COSY and ROESY correlations were observed between an olefinic methine resonance at δ 5.38, assigned to H-2, and a broad two proton singlet at δ 4.46, assigned to the H-15 methylene protons. HMBC correlations were observed between a carbonyl resonance at δ 169.9 and both the H-15 methylene proton resonance at δ 4.46 and a singlet methyl resonance at δ 1.97. These HMBC correlations demonstrated that in caribaeolin (**7**) a C-15 acetyl substituent was present in place of the C-15 arabinose sugar residue found in caribaeoside (**6**). Strong ROESY correlations were observed between the Me-17 resonance at δ 0.77 and the H-2 olefinic proton resonance at δ 5.38, indicating that Me-17 and C-2 were cis to each other as in caribaeoside (**6**). Additional ROESY correlations observed between the C-19/C-20 isopropyl methyl proton resonances at δ 0.95−0.96 and the H-1 (δ 4.01) and H-10 (δ 2.07) resonances, between the Me-16 (δ 1.34) and both of the H-8 (δ 4.85) and OMe-21 (δ 3.08) resonances, and between the H-8 and H-10 (δ 2.07) resonances confirmed that the relative sterochemistry in caribaeolin (**7**) was the same as in caribaeoside (**6**).

All of the *E. caribaeorum* diterpenoids **1−7** reported above showed antimitotic activity in the cell-based assay.[7] Desmethyleleutherobin (**2**) (IC$_{50}$ 20 nM) and isoeleutherobin A (**4**) (IC$_{50}$ 50 nM) were both slightly more potent than eleutherobin (**1**) (IC$_{50}$ 100 nM), Z-eleutherobin (**5**) (IC$_{50}$ 250 nM) was comparable in activity to eleutherobin (**1**), desacetyleleutherobin (**3**) (IC$_{50}$ 400 nM) was slightly less potent, while caribaeoside (**6**) (IC$_{50}$ 20 μM) and caribaeolin (**7**) (IC$_{50}$ 20 μM) were considerably less potent that eleutherobin (**1**).

Many synthetic analogues of eleutherobin (**1**) have been prepared as part of SAR studies;[10] however, to date they have

all been based on the eleutherobin diterpenoid core. The Ojima pharmacophore proposal implies that changes in the C-11−C-13 region of eleutherobin should have an impact on the ability of analogues to stabilize tubulin polymers. Caribaeoside (**6**) represents the first such analogue to be tested for antimitotic activity. The significant decrease in antimitotic potency of caribaeoside (**6**) relative to eleutherobin (**1**), resulting from introduction of a hydroxyl group at C-11 and migration of the olefin to the $\Delta^{12,13}$ position, provides further support for Ojima's pharmacophore model. The structural changes in **6** alter both the shape and polarity of the diterpene core in the tubulin binding region B of the proposed pharmacophore.

A number of other features of the antimitotic potencies are also noteworthy. Altering the $\Delta^{2′,3′}$ configuration (i.e., **5**), a change in the A region of the pharmacophore, has little effect, while alterations in the arabinose fragment, representing changes in the C region of the pharmacophore, can either enhance (i.e., **4**) or decrease (i.e., **3**) the potency. Changing the C-4 substituent from methoxyl (i.e., **1**) to hydroxyl (i.e., **2**), an alteration that is formally outside of the Ojima pharmacophore binding regions, leads to a slight increase in potency. Replacement of the arabinose fragment in caribaeoside (**6**) with a simple acetate residue (i.e., **7**) results in no additional loss of potency, which is consistent with previous observations.[6]

In summary, the current study has identified a new and relatively high-yielding source of eleutherobin (**1**), whose preclinical development has been impeded by its scarcity, as well as providing a series of new eleutherobin analogues **2−7** that serve as a further test of recent pharmacophore models for microtubule stabilization.

Supporting Information Available: Tables of optical rotations, UV data, and ^1H and ^{13}C NMR assignments for compounds **1−8**. This material is available free of charge via the Internet at http://pubs.acs.org.

OL9912027

(10) (a) McDaid, H. M.; Bhattacharya, Chen, X.-T.; He, L.; Shen, H.-J.; Gutteridge, C. E.; Horowitz, S. B.; Danishefsky, S. J. *Cancer Chemother. Pharmacol.* **1999**, *44*, 131−137. (b) Nicolaou, K. C.; Winssinger, N.; Vourloumis, D.; Ohshima, T.; Kim, S.; Pfefferkorn, J.; Xu, J.-Y.; Li, T. *J. Am. Chem. Soc.* **1998**, *120*, 10814−10826.

Solid-state and solution conformations of eleutherobin obtained from X-ray diffraction analysis and solution NOE data

Bruno Cinel,[a] Brian O. Patrick,[b] Michel Roberge[c] and Raymond J. Andersen[a,*]

[a]Departments of Chemistry and Earth and Ocean Sciences, University of British Columbia, Vancouver BC V6T 1Z1, Canada
[b]Department of Chemistry, University of British Columbia, Vancouver BC V6T 1Z1, Canada
[c]Department of Biochemistry and Molecular Biology, University of British Columbia, Vancouver BC V6T 1Z3, Canada

Abstract

Single crystal X-ray diffraction analysis has revealed the solid-state conformation of the microtubule-stabilizing diterpenoid eleutherobin (1). NOE data obtained for **1** in $CDCl_3$ and DMSO-d_6 are consistent with solution conformations that are virtually identical to the solid state conformation. © 2000 Elsevier Science Ltd. All rights reserved.

Eleutherobin (**1**), initially isolated from a Western Australian octocoral in the genus *Eleutherobia* (possibly *albiflora*), represents one of a small number of antimitotic natural product families that are known to stabilize microtubules.[1] Other structural types possessing this important biological activity are represented by paclitaxel,[2] epothilones A and B,[3] discodermolide,[4] and the laulimalides.[5] The current excitement surrounding this group of compounds stems from the FDA approval of paclitaxel for the treatment of ovarian (1992) and metastatic breast cancers (1994). Paclitaxel's clinical utility has generated great interest in developing additional anticancer drug candidates that exploit its mechanism of action. One approach to designing the next generation of microtubule-stabilizing compounds has been to create three-dimensional pharmacophore models that embrace all the available SAR data for the known natural product structural types with these properties.[6,7] The validity of this approach has been demonstrated by the pharmacophore-guided design and subsequent synthesis of new hybrid structures with demonstrated cytotoxic and tubulin binding abilities.[6]

Creation of predictive pharmacophore models depends on detailed knowledge about the conformation of all the known structural types possessing microtubule stabilizing properties. To date, there have been no published solid-state or solution conformational analyses of eleutherobin (**1**), although the original report of the structure elucidation did provide a series of useful NOE constraints. Recently, we discovered that the Caribbean octocoral *Erythropodium caribaeorum* is a relatively high-yielding source

---

* Corresponding author. Tel: 604 822 4511; Fax: 604 822 6091; e-mail: randersn@unixg.ubc.ca (R. J. Andersen)

of eleutherobin and several new structural analogs.[8] During the course of characterizing the antimitotic diterpenes from the *E. caribaeorum* extracts, several crystals of eleutherobin (**1**) were obtained by the fortuitous slow evaporation of a concentrated NMR sample dissolved in DMSO-d_6. The crystals proved to be suitable for X-ray diffraction analysis, which has provided the first solid state conformation for eleutherobin (**1**). ROESY and difference NOE data have also been collected for eleutherobin (**1**) in DMSO-d_6 and CDCl$_3$ in order to facilitate a comparison of the solid state conformation with the solution conformations in both a polar and a nonpolar solvent.

Eleutherobin (**1**) crystallized in space group $P2_12_12_1$ with a=12.8291(8), b=13.6209(6), and c=19.168(1) Å. A crystal with dimensions 0.30×0.20×0.15 mm, was mounted on a glass fiber. Data were collected at –100°C on a Rigaku/ADSC CCD area detector in two sets of scans (ϕ=0.0 to 190.0°, χ=0°; and ω=–18.0 to 23.0°, χ=–90°) using 0.50° oscillations with 58.0 s exposures. The crystal-to-detector distance was 40.55 mm with a detector swing angle of –5.52°. Of the 7035 unique reflections measured (Mo-Kα radiation, $2\theta_{max}$=55.8°, R_{int}=0.071, Friedels not merged), 4520 were considered observed (I>3$\sigma(I)$). The final refinement residuals were R=0.046 (on F, I>3$\sigma(I)$) and $wR2$=0.141 (on F^2, all data).[9] The data was processed using the d*TREK program and corrected for both Lorentz and polarization effects. The structure was solved by direct methods[10] and all non-hydrogen atoms were refined anisotropically, while all hydrogens involved in hydrogen-bonding were refined isotropically. All other hydrogens were included in calculated positions. The enantiomorph shown in Fig. 1 was chosen based on the known configuration of eleutherobin (**1**).[11] All calculations were performed using the teXsan[12] crystallographic software package of the Molecular Structure Corporation.
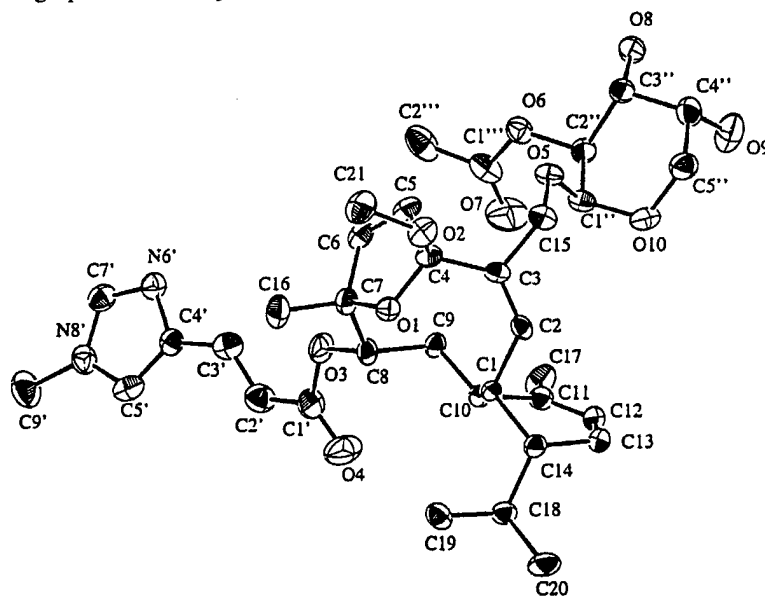

Fig. 1. ORTEP drawing of eleutherobin (**1**). Hydrogen atoms have been omitted for clarity

ROESY (500 MHz) and difference NOE (400 MHz) data were collected for eleutherobin (**1**) dissolved in DMSO-d_6 and CDCl$_3$. The NMR samples were degassed and purged of oxygen by freezing in a dry ice/acetone bath and placing the frozen sample under vacuum. The degassed samples were then flushed with argon and sealed. Table 1 lists the difference NOE results obtained in CDCl$_3$ and the ROESY

correlations observed in $CDCl_3$ and DMSO-d_6 along with the solid-state internuclear distances between the relevant pairs of protons. A number of key NOEs indicate that the solution conformation of the diterpenoid core of eleutherobin (1) in both $CDCl_3$ and DMSO-d_6 is identical to, or at least extremely similar to, the solid state conformation. These include difference NOEs observed in the resonances for H1, H10, and Me19 when the H8 resonance is irradiated and in H13α when H2 is irradiated. The C8–C9–C10–C1 torsional angle in the solid state is −66°, which places H8 2.438 Å from H1 and 2.304 Å from H10, consistent with the difference NOEs observed. A C9–C10–C1–C14 torsional angle of 177.7° in the solid state brings the Me19 protons into sufficient proximity to H8 to explain the weak difference NOE observed between their resonances, and the C2–C1–C14–C13 torsional angle of −61° in the solid state places H2 only 2.118 Å from H13α in agreement with the strong difference NOE observed between their resonances. Molecular models indicate that the combination of H8 to H10, H1, Me19 and H2 to H13α NOEs represent an extremely restrictive set of conformational constraints. Any significant deviation from the solid–state conformation results in H8 to H1, H10, Me19 and H2 to H13α interproton distances that would make the simultaneous appearance of the observed suite of NOEs between these protons highly unlikely. The diagnostic dipolar couplings between H8 and both H1 and H10, and between H2 and H13α, are all observed as ROESY correlations in both $CDCl_3$ and DMSO-d_6, providing additional evidence that the solution conformations in both solvents must be essentially identical to the solid-state conformation.

Table 1

Difference NOE[a] and ROESY[b] data for eleutherobin (1) in $CDCl_3$ and DMSO-d_6

H# (δ in $CDCl_3$)	H# (δ in $CDCl_3$)	Internuclear Distance from X-ray Data (Å)	Difference NOE (% enhancement) H in First Column was Irradiated	ROESY Correlations in $CDCl_3$	ROESY Correlations in DMSO-d_6
H2 (5.54)	H13α (2.29)[c]	2.12	7.49	y	y
H2	H14 (1.21)	2.61	3.51	y	y
H8 (4.80)	H1 (3.94)	2.44	4.28	y	y
H8	H10 (2.60)	2.30	6.16	y	y
H8	H16 (1.43)	2.52	0.91	y	y
H8	H19 (0.96)	2.64	0.52	y	n
H10 (2.60)	H1 (3.94)	2.33	4.79	y	y
H10	H8 (4.80)	2.30	2.61	y	y
H10	H19 (0.96)	2.51	0.77	n	n
H13α (2.29)[c]	H2 (5.54)	2.12	9.69	y	y
H14 (1.21)	H1 (3.94)	2.37	6.40	y	y
H19 (0.96)	H1	2.02	0.97	y	y
H19	H8 (4.80)	2.64	0.32	y	n
H19	H10 (2.60)	2.51	0.42	n	n
H20 (0.94)	H13β (1.97)[c]	2.03	0.96	y	y
OMe (3.20)	H16 (1.43)	2.28	1.01	y	y

[a] 400 MHz; [b] 500 MHz; [c] β and α are defined as being above and below the plane of the diterpenoid core of eleutherobin in the structural representation 1; n – ROESY correlation not clear; y – ROESY correlation clearly observed.

It is interesting to compare the conformation of eleutherobin (1) revealed by the X-ray diffraction and solution NOE data in the current study to the conformation used by Ojima et al. in constructing their common pharmacophore for microtubule-stabilizing natural products.[6] In order to generate a

conformation for pharmacophore creation, Ojima et al. carried out molecular dynamic calculations on eleutherobin (1) without using any constraints. The exact coordinates for the resulting conformation that they used for 1 were not available, but Figure 4 in their paper indicates that the modeled conformation had a C8–C9–C10–C1 torsional angle of $>-90°$ and a C2–C1–C14–C13 torsional angle approaching 180°. A conformation with those torsional angles would not be expected to give any of the NOEs that are observed between H8 and H1 and Me19, or between H2 and H13α in CDCl$_3$ and DMSO-d_6. The Ojima conformation gives their binding region B (C11–C12–C13) a much different spatial relationship relative to the A (uroconic acid side chain) and C (D-arabinose residue) binding regions compared to the solid-state conformation (see Scheme 1). This suggests that the solid-state and solution conformations of eleutherobin (1) determined herein might have significantly different overlay fits with the reference structure nonataxel and the other microtubule-stabilizing structures that were used to construct the common pharmacophore. Therefore, it is anticipated that the availability of solid-state and solution conformation data for eleutherobin (1) will facilitate further refinements of microtubule-stabilizing pharmacophore models and, consequently, aid the eventual design of new compounds with this important biological activity.
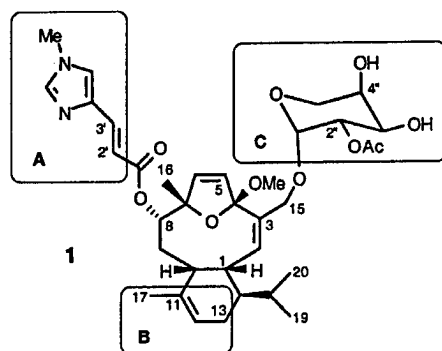
Scheme 1.

Acknowledgements

References

1. (a) Lindel, T.; Jensen, P. R.; Fenical, W.; Long, B. H.; Casazza, A. M.; Carboni, J.; Fairchild, C. R. *J. Am. Chem. Soc.* **1997**, *119*, 8744–8745. (b) Long, B. H.; Carboni, J. M.; Wasserman, A. J.; Cornell, L. A.; Casazza, A. M.; Jensen, P. R.; Lindel, T.; Fenical, W.; Fairchild, C. R. *Cancer Res.* **1998**, *58*, 1111–1115.
2. Baloglu, E.; Kingston, D. G. I. *J. Nat. Prod.* **1999**, *62*, 1448–1472.
3. Bollag, D. M.; McQueney, P. A.; Zhu, J.; Hensens, O.; Koupal, L.; Liesch, J.; Geotz, M.; Lazarides, E.; Woods, C. M. *Cancer Res.* **1995**, *55*, 2325–2333.

4. ter Haar, E.; Kowalski, R. J.; Hamel, E.; Lin, C. M.; Longley, R. E.; Gunasekera, S. P.; Rosenkranz, H. S.; Day, B. W. *Biochemistry* **1996**, *35*, 243–250.
5. Mooberry, S. L.; Tien, G.; Hernadez, A. H.; Plubrukarn, A.; Davidson, B. S. *Cancer Res.* **1999**, *59*, 653–660.
6. Ojima, I.; Chakravarty, S.; Inoue, T.; Lin, S.; He, L.; Horwitz, S. W.; Kuduk, S. D.; Danishefsky, S. J. *Proc. Natl. Acad. Sci., USA* **1999**, *96*, 4256–4261.
7. Wang, W.; Xia, X.; Kim, Y.; Hwang, D.; Jansen, J. M.; Botta, M.; Liotta, D. C.; Snyder, J. P. *Org. Lett.* **1999**, *1*, 43–46.
8. Cinel, B.; Roberge, M.; Behrisch, H.; van Ofwegen, L.; Castro, C. B.; Andersen, R. J. *Org. Lett.* **2000**, *2*, 257–260.
9. Archival crystallographic data have been deposited with the Cambridge Crystallographic Data Centre, University Chemical Laboratory, Lensfield Road, Cambridge CB2 1EW, UK. Please give a complete literature citation when ordering.
10. Altomare, A.; Cascarano, M.; Giacovazzo, C.; Guagliardi, A. *J. Appl. Cryst.,* **1993**, *26*, 343–350.
11. Chen, X.-T.; Bhattacharya, S. K.; Zhou, B.; Gutteridge, C. E.; Pettus, T. R. R.; Danishefsky, S. J. *J. Am. Chem. Soc.* **1999**, *121*, 6563–6579.
12. Crystal Structure Analysis Package, Molecular Structure Corporation (1985 and 1992).

Antimitotic diterpenoids from *Erythropodium caribaeorum*: isolation artifacts and putative biosynthetic intermediates
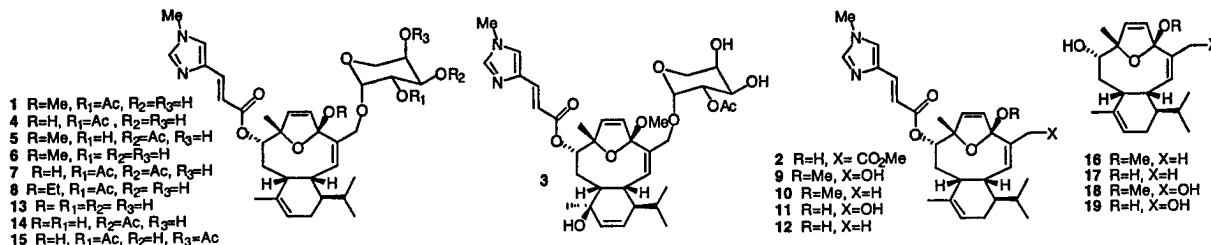
Robert Britton,[a] Michel Roberge,[b] Hans Berisch[c] and Raymond J. Andersen[a],*

[a]*Departments of Chemistry and Oceanography (EOS), University of British Columbia, Vancouver, BC, Canada V6T 1Z1*
[b]*Department of Biochemistry and Molecular Biology, University of British Columbia, Vancouver, BC, Canada V6T 1Z3*
[c]*Ross University Medical School, Commonwealth of Dominica*

Abstract—Two new natural products, caribaeorane (**12**) and 15-hydroxycaribaeorane (**11**), have been identified in *Erythropodium caribaeorum* extracts by isolation of their C-4 methylketals **10** and **9**. It has been demonstrated that eleutherobin (**1**) is an isolation artifact. A proposal for the late stages of the biosynthetic pathway to the *E. caribaeorum* antimitotic diterpenoids is presented. © 2001 Published by Elsevier Science Ltd.

Eleutherobin (**1**), isolated by Fenical and coworkers from the Western Australian soft coral *Eleutherobia* sp., belongs to a small family of soft coral diterpenoids that are microtubule-stabilizing antimitotic agents.[1] A large amount of effort has been directed towards the total synthesis of eleutherobin and other members of this family.[2] Although these efforts have culminated in the total synthesis of eleutherobin (**1**), its preclinical evaluation as an anticancer drug has been stalled by the limited supply of material available for testing.[3] Recently, we reported that the relatively abundant Caribbean soft coral *Erythropodium caribaeorum* is a good source of eleutherobin (**1**) and a number of analogs including sarcodictyin A (**2**), caribaeoside (**3**), Z-eleutherobin, desmethyleleutherobin (**4**), isoeleutherobin A (**5**), and desacetyleleutherobin (**6**).[4,5] *E. caribaeorum* could provide adequate quantities of material for preclinical evaluation of this promising family of anticancer drug leads and even clinical trials should the compounds progress that far.

Initial collections of *E. caribaeorum* examined by our laboratory were extracted with MeOH, resulting in the isolation of highly variable ratios of eleutherobin (**1**) and desmethyleleutherobin (**4**). Ketzinel et al. have reported isolating the eleuthosides (e.g. **7**), which are all hemiketals at C-4, from *Eleutherobia aurea* by using non-alcohol solvents such as EtOAc.[6] These observations raised the possibility that eleutherobin (**1**) was actually an isolation artifact. To resolve this issue, fresh specimens of *E. caribaeorum* were collected in Dominica and one portion of the sample was extracted with EtOH and a second portion was extracted with MeOH. The MeOH extracted sample yielded eleutherobin (**1**), desmethyleleutherobin (**4**), and sarcodictyin A (**2**) as the major components along with minor amounts of **3**, **5**, and **6** as before,[5] while the EtOH extracted sample yielded the C-4 ethylketal **8** along with **2** and **4** as the major components. Eleutherobin (**1**) could not be detected by analytical HPLC or NMR analysis of the chromatography fractions from the EtOH extract.

1 R=Me, R₁=Ac, R₂=R₃=H
4 R=H, R₁=Ac, R₂=R₃=H
5 R=Me, R₁=H, R₂=Ac, R₃=H
6 R=Me, R₁= R₂=R₃=H
7 R=H, R₁=Ac, R₂=Ac, R₃=H
8 R=Et, R₁=Ac, R₂= R₃=H
13 R= R₁=R₂= R₃=H
14 R=R₁=H, R₂=Ac, R₃=H
15 R=H, R₁=Ac, R₂=H, R₃=Ac

3

2 R=H, X= CO₂Me
9 R=Me, X=OH
10 R=Me, X=H
11 R=H, X=OH
12 R=H, X=H

16 R=Me, X=H
17 R=H, X=H
18 R=Me, X=OH
19 R=H, X=OH

* Corresponding author.

These results show that the C-4 methyl ketal in eleutherobin (1) isolated from *E. caribaeorum* is indeed an artifact.

During the course of fractionating a large scale *E. caribaeorum* MeOH extract in order to obtain sufficient eleutherobin (1) for biological testing, the eleutherobin aglycon 9[7] and methylcaribaeorane (10) were isolated as very minor components along with sarcodictyin A (2) from the least polar fractions eluting from silica gel with EtOAc:MeOH (85:15). The eleutherobin aglycon 9 has previously been reported as a synthetic intermediate.[2a] Comparison of the spectroscopic data collected on the material isolated from *E. caribaeorum*[7] with the literature data for the synthetic compound confirmed that they were identical. The eleutherobin aglycon 9 is presumed to be an artifact formed from the corresponding hemiketal natural product 15-hydroxycaribaeorane (11) during the MeOH extraction.

Methylcaribaeorane (10),[8] isolated as a white amorphous solid, gave an [M+H]+ ion at *m/z* 467.2912 in the HRFABMS appropriate for a molecular formula of $C_{28}H_{38}N_2O_4$ that differed from the molecular formula of the eleutherobin aglycon 9 simply by the loss of one oxygen atom. Examination of the ^{1}H and ^{13}C NMR data obtained for methylcaribaeorane (10) revealed the presence of two olefinic methyl groups (^{1}H NMR, C_6D_6: δ 1.65, s, 3H; 1.80, s, 3H) and the absence of resonances that could be assigned to an allylic hydroxymethyl fragment. These observations indicated that methylcaribaeorane (10) was simply missing the C-15 allylic alcohol found in the eleutherobin aglycon 9. HMBC correlations observed between a methyl resonance at δ 3.18 and a carbon resonance at δ 117.4 assigned the carbon resonance to the C-4 ketal. The olefinic methyl resonance at δ 1.80 showed HMBC correlations to the C-4 ketal carbon resonance at δ 117.4 and to the C-2 and C-3 olefinic carbon resonances at δ 131.3 and 134.0, respectively, confirming that there was an allylic methyl at C-15. The remaining NMR data for methylcaribaeorane was completely consistent with the structure 10.[8] Methylcaribaeorane (10) is also presumed to be an isolation artifact formed from the corresponding hemiketal natural product caribae-

orane (12). The eleutherobin aglycon 9 and methylcaribaeorane (10) were active in a cell-based assay for antimitotic activity at 1 and 10 µM, respectively.[5]

Most of the compounds isolated from the *E. caribaeorum* MeOH extract had C-4 methylketals, which are artifacts. Interestingly, sarcodictyin A (2) was only isolated as the C-4 hemiketal. Since methylketal transformations clearly take place during the extraction process, it seemed possible that the eleutherobin aglycon 9 might also be an artifact formed from eleutherobin (1) by hydrolysis/methanolysis of the glycosidic linkage during extraction. An investigation of the ketal transformations was undertaken in order to confirm that glycoside hydrolysis was not occurring during extraction and to gain insight into the lack of ketal formation in sarcodictyin A (2). First, it was found that desmethyleleutherobin (4) can be converted quantitatively to eleutherobin (1) by treatment with a catalytic amount of pyridinium *p*-toluenesulfonate (PPTS) in methanol at room temperature.[2] The reverse transformation, 1 to 4, can be quantitatively effected using PPTS and water/CH_2Cl_2. Neither of these transformations result in glycoside hydrolysis. Saracodictyin A (2) could also be converted quantitatively to its methylketal using PPTS and MeOH at rt. The combination of the extraction and the laboratory observations indicate that the MeOH extraction conditions are able to readily convert the C-4 hemiketal to the methylketal when there is a methyl, hydroxymethyl, or glycosidic functionality at C-15, but that they cannot effect methylketal formation when there is a ester at C-15. The PPTS in MeOH or PPTS in water/CH_2Cl_2 quantitatively interconverts all C-4 hemiketals and methylketals, but still does not bring about glycoside hydrolysis. Therefore, it is apparent that the milder MeOH extraction conditions will not cleave the glycoside linkage, confirming that 15-hydroxycaribaeorane (11) is indeed a natural product.

The discovery of methylcaribaeorane (10) and the eleutherobin aglycon 9 as minor constituents in the MeOH extracts of *E. caribaeorum* along with the previously reported compounds 1 to 6, and the demonstration that the C-4 methyl ketal functionalities in these
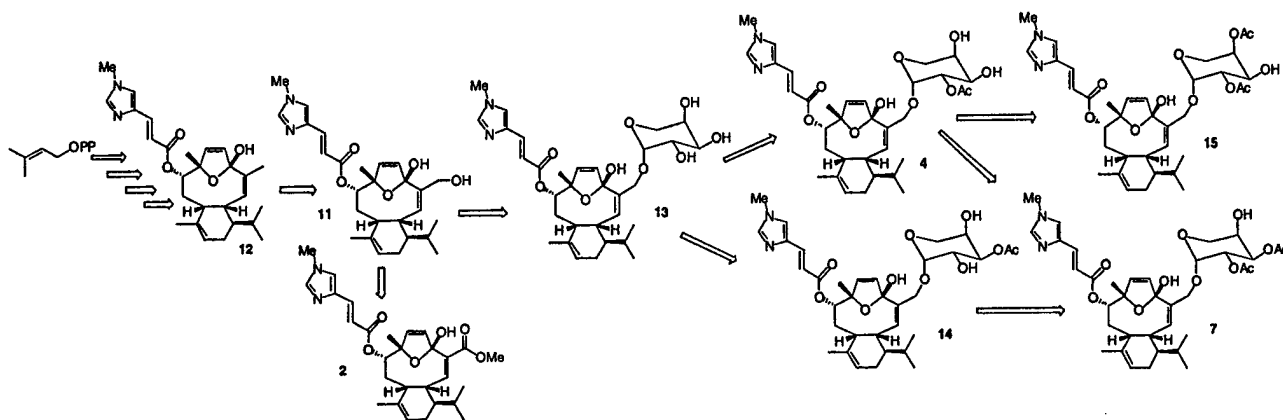
Scheme 1.

compounds are isolation artifacts, led to the biosynthetic proposal presented in Scheme 1. This proposal suggests that geranylgeranylpyrophosphate undergoes cyclization and oxidative functionalization to give the diterpenoid core which is esterified at the C-8 hydroxyl with the urocanic acid residue to give caribaeorane (12), the first known intermediate in the pathway. Caribaeorane (12) would then be oxidized to 15-hydroxycaribaeorane (11) and the arabinose residue would be added to give desacetyldesmethyleleutherobin (13), which if monoacetylated at C-2′ would give desmethyleleutherobin (4) or at C-3′ would give desmethylisoeleutherobin A (14). Further acetylation of either 4 or 14 would give eleuthoside A (7), while acetylation of desmethyleleutherobin (4) at C-4′ would give eleuthoside B (15). In this proposal, sarcodictyin A (2) represents a shunt metabolite formed by further oxidation of 15-hydroxycaribaeorane (11) to the 15-carboxylic acid followed by SAM methylation to give the methyl ester. It should be noted that there is no evidence for the occurrence of either 7 or 15 in the *E. caribaeorum* extract, however, their biosynthesis in *Eleutherobia aurea* would presumably follow the same pathway.

One significant aspect of the hypothesis presented in Scheme 1 is the proposal that the urocanic ester residue is added to the diterpenoid core before the C-15 alcohol required for glycoside formation is introduced. In an attempt to provide further evidence for this suggestion, the urocanic acid residue was removed from methylcaribaeorane (10) by hydrolysis with a few drops of 5N NaOH in MeOH overnight at rt to give 16,[9] the methyl ketal analog of one of the potential biosynthetic precursors 17 of caribaeorane (12). Careful examination of the *E. caribaeorum* MeOH extract chromatography fractions by TLC and GC analysis using 16 as a reference failed to show any evidence for its presence. The corresponding hydrolysis product 18[10] of the eleutherobin aglycon 9 was also prepared and once again TLC and GC analysis failed to show any evidence for its presence in the *E. caribaeorum* MeOH extract. This negative evidence does not eliminate 17 as the immediate biosynthetic precursor to caribaeorane (12) or rule out the possibility that 19 is the direct precursor to 11, but it does raise the interesting possibility that the urocanic ester is formed before all the diterpenoid functionality, such as the C-7 tertiary alcohol or the C-4 ketone, are in place.

Acknowledgements

References

1. Lindel, T.; Jensen, P. R.; Fenical, W.; Long, B. H.; Casazza, A. M.; Carboni, J.; Fairchild, C. R. *J. Am. Chem. Soc.* **1997**, *119*, 8744–8745.
2. (a) Nicolaou, K. C.; Xu, J.-X.; Kim, S.; Oshima, T.; Hosokawa, S.; Pfefferkorn, J. *J. Am. Chem. Soc.* **1997**, *119*, 11353–11354; (b) Chen, X.-T.; Bhattacharya, S. K.; Zhou, Z.; Gutteridge, C. E.; Pettus, T. R. R.; Danishefsky, S. J. *J. Am. Chem. Soc.* **1999**, *121*, 6563–6579; (c) Nicolaou, K. C.; Ohshima, T.; Hosokawa, S.; van Delft, F. L.; Vourloumis, D.; Xu, J. Y.; Pfefferkorn, J.; Kim, S. *J. Am. Chem. Soc.* **1998**, *120*, 8674–8680.
3. Rayl, A. J. S. *The Scientist* **1999**, *13*, 1–3.
4. Cinel, B.; Roberge, M.; Behrisch, H.; van Ofwegen, L.; Castro, C. B.; Andersen, R. J. *Org. Lett.* **2000**, *2*, 257–260.
5. Roberge, M.; Cinel, B.; Anderson, H. J.; Lim, L.; Jiang, X.; Xu, L.; Kelly, M. T.; Andersen, R. J. *Cancer Res.* **2000**, *60*, 5052–5058.
6. Ketzinel, S.; Rudi, A.; Schleyer, M.; Benayahu, Y.; Kashman, Y. *J. Nat. Prod.* **1996**, *59*, 873–873.
7. Eleutherobin aglycon 9: ^{1}H NMR (CDCl$_3$, 400 MHz) δ 7.52, d, $J=15.4$ Hz (H-3′), 7.45, s (H-7′), 7.08, s (H-5′), 6.54, d, $J=15.4$ Hz (H-2′), 6.21, d, $J=6.0$ Hz (H-6), 6.02, d, $J=6.0$ Hz (H-5), 5.56, d, $J=9.4$ Hz (H-2), 5.25, m (H-12), 4.80, d, $J=7.4$ Hz (H-8), 4.16, d, $J=12.0$ Hz (H-15), 3.85–3.95, m (H-15, H-1), 3.69, s (H-9′), 3.23, s (H-21), 2.67, m (OH), 2.59, m (H-10), 2.31, m (H-13), 1.98, m (H-13), 1.50–1.65, m (H-9, H-18), 1.50, s (H-17), 1.45, s (H-16), 1.25–1.40, m (H-9, H-14), 0.97, d, $J=6.5$ Hz (H-19), 0.91, d, $J=6.5$ Hz (H-20); HRFABMS [M+H]$^+$ calcd for C$_{28}$H$_{39}$N$_2$O$_5$: 483.2859, found: 483.2860; $[\alpha]_D$ −24.2°.
8. Methylcaribaeorane (10): ^{1}H NMR (C$_6$D$_6$, 500 MHz) δ 7.95, d, $J=15.4$ Hz (H-3′), 7.26, d, $J=15.4$ Hz (H-2′), 6.72, s (H-7′), 6.00, s (H-5′), 5.95, d, $J=5.8$ Hz (H-6), 5.78, d, $J=5.8$ Hz (H-5), 5.49, d, $J=9.7$ Hz (H-2), 5.33, m (H-12), 5.25, d, $J=7.3$ Hz (H-8), 4.30, m (H-1), 3.18, s (H-21), 2.95, m (H-10), 2.37, m (H-13), 2.25, s (H-9′), 2.00, m (H-9), 1.98, m (H-13), 1.81, m (H-9), 1.80, s (H-15), 1.65, s (H-17), 1.57, m (H-18), 1.46, s (H-16), 1.28, m (H-14), 1.06, d, $J=6.5$ Hz (H-19), 0.89, d, $J=6.5$ Hz (H-20); ^{13}C NMR (C$_6$D$_6$, 100 MHz) δ 167.1 (C-1′), 139.2 (C-4′), 139.2 (C-7′), 137.3 (C-3′), 134.9 (C-11), 134.8 (C-6), 134.0 (C-3), 131.3 (C-2), 130.1 (C-5), 122.6 (C-5′), 121.6 (C-12), 117.4 (C-4), 116.5 (C-2′), 90.5 (C-7), 82.2 (C-8), 49.5 (C-21), 43.3 (C-14), 39.6 (C-10), 34.6 (C-1), 32.3 (C-9), 31.9 (C-9′), 29.4 (C-18), 24.9 (C-16), 24.8 (C-13), 22.4 (C-15), 22.3 (C-17), 22.2 (C-20), 20.8 (C-19); HRFABMS [M+H]$^+$ calcd for C$_{28}$H$_{39}$N$_2$O$_4$: 467.2910, found: 467.2912.
9. Compound 16: ^{1}H NMR (C$_6$D$_6$, 400 MHz) δ 5.99, d, $J=5.9$ Hz (H-6), 5.74, d, $J=5.9$ Hz (H-5), 5.41, dd, 1H, $J=9.3$, 1.3 Hz (H-2), 5.36, m (H-12), 4.15, m (H-1), 3.47, m (H-8), 3.19, s (H-21), 2.35, m (H-10), 2.28, m (H-13), 1.97, m (H-13), 1.80, s (H-15), 1.62, s (H-17), 1.50, s (H-16), 1.50–1.72, m (H-9, H-18, H-14, OH), 1.27, m (H-9), 0.98, d, $J=6.5$ Hz (H-19), 0.93, d, $J=6.5$ Hz (H-20); HRDCI$^+$MS calcd for C$_{21}$H$_{32}$O$_3$: 332.2351, found: 332.2351.

10. Compound **18**: ^{1}H NMR (C_6D_6, 400 MHz) δ 5.94, d, $J=5.9$ Hz (H-6), 5.68, d, $J=5.9$ Hz (H-5), 5.67, d, $J=9.5$ Hz (H-2), 5.31, m (H-12), 4.00–4.20, m (H-1, H-15, H-15), 3.44, bd, $J=6.1$ Hz (H-8), 3.00, s (H-21), 2.23–2.38, m (OH, H-10, H-13), 1.93, m (H-13), 1.59, s (H-17), 1.43, s (H-16), 1.42–1.62, m (H-9, H-18, OH), 1.30, m (H-14), 1.25, m (H-9), 0.93, d, $J=6.9$ Hz (H-19), 0.90, d, $J=6.7$ Hz (H-20); HRDCI$^+$MS calcd for $C_{21}H_{32}O_4$: 348.2301, found: 348.2303.

Synthetic Transformations of Eleutherobin Reveal New Features of its Microtubule-Stabilizing Pharmacophore

Robert Britton,[†] E. Dilip de Silva,[†] Cristina M. Bigg,[¥] Lianne M. McHardy,[¥] Michel Roberge,[¥] and Raymond J. Andersen*[†]

[†]Departments of Chemistry and EOS, University of British Columbia, Vancouver, B.C., Canada, V6T 1Z1; [¥]Department of Biochemistry and Molecular Biology, University of British Columbia, Vancouver, B.C., Canada, V6T 1Z3

The clinical usefulness of paclitaxel for treating cancer has generated significant interest in finding other compound classes that stabilize microtubules. Discodermolide, epothilones, laulimalide, and the eleuthesides also have this important biological property.[1] Several pharmacophore models have attempted to reconcile the SAR data for the taxoids and other compound types in order to generate a sufficiently detailed understanding of the tubulin binding requirements to allow rational design of new classes of microtubule-stabilizing drugs.[2] The predictive power of the pharmacophore models relies on accurate knowledge of the structural features required for activity in each compound class.

Eleutherobin (1), isolated by Fenical et al. from the rare alcyonacean *Eleutherobia* sp., belongs to the 'eleutheside' family of microtubule-stabilizing diterpenoids.[3] Total syntheses of eleutherobin and related eleuthesides[4] has provided information about the nature of the C-8 ester, the C-4 ketal, and the C-15 functionality required for strong interaction of eleuthesides with tubulin, which has facilitated the incorporation of this diterpenoid template into pharmacophore models.[2] However, neither synthesis nor the original natural source has provided sufficient quantities of eleutherobin to permit full *in vivo* evaluation and this has thwarted its further development.

The Caribbean soft coral *Erythropodium caribaeorum* was recently found to be a good source of eleuthesides.[5] Eleutherobin (1) can be obtained directly as an isolation artifact from MeOH extracts of *E. caribaeorum* or by chemical transformation of desmethyleleutherobin (2), the major

eleutheside in the soft coral.[5c] The ready availability of 1 has led to the determination of its solid-state and solution conformations,[6] paved the way for *in vivo* testing, and created an opportunity to investigate chemical transformations of the molecule. In this communication, we report the first detailed investigation of the reactivity of intact eleutherobin, which has uncovered some striking and unanticipated features of its antimitotic pharmacophore.

The total syntheses of eleuthesides have generated very limited diversity in the diterpenoid core, with major variations reported only in the C-15 functionality.[4] Nevertheless, all of the pharmacophore models suggest, without supporting data other than structural overlays, that the cyclohexene ring and its appended substituents (i.e. the isopropyl residue) are important determinants of antimitotic activity. There is also general agreement that the urocanic ester is crucial and the Giannakakou model[2a] suggests that the C-4/C-7 ether bridge in 1 is a hydrogen bond acceptor corresponding to the oxetane oxygen in the taxoids and to the 12,13 epoxide in the epothilones. The importance of the cyclohexene ring is supported by the observation that caribaeoside, which has a β-hydroxyl at C-11 and a $\Delta^{12,13}$ olefin, is ≈ 1,000-fold less active than eleutherobin.[5a] Prompted by the potential importance of the C-4/C-7 ether bridge, the urocanic ester, and the cyclohexene ring for antimitotic activity in the eleuthesides, our chemical transformations focussed on the masked C-4 ketone and olefin oxidation/reduction reactions.
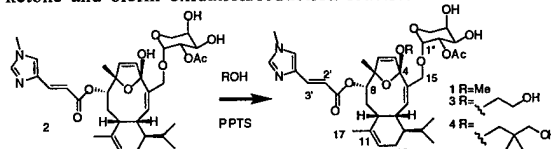
Scheme 1

The first objective was to trap the C-4 ketone in 1 as a cyclic ketal in order to liberate the C-4/C-7 ether oxygen as a C-7 alcohol and to change the oxygen atom's spatial relationship with the C-14 isopropyl group. In order to test the reactivity of the C-4 hemiketal, desmethyleleutherobin (2) was treated with various neat aliphatic alcohols (ROH: R = Et, ⁿPr, ⁿBu, ⁱPr) and excess PPTS at rt, which gave the corresponding C-4 ketal analogs in excellent yield (Scheme 1). Attempts to make the C-4 cyclic ketals of 2 with ethylene glycol or 2,2-dimethyl-1,3-propanediol under a variety of conditions using PPTS as a catalyst gave only 3 and 4. The x-ray structure of eleutherobin[6] shows significant distortion of the C-1/C-2/C-3 (132°) and C-2/C-3/C-4 (127°) bond angles. This angle strain may act like a clamp to keep the dihydrofuran ring from opening during the transketalization reactions.

Next we turned our attention to oxidation reactions involving the $\Delta^{11,12}$ olefin. Reaction of 1 with MCPBA in CH_2Cl_2 at rt for 8 h gave a mixture of two epoxides, 5 and 6 (Scheme 2). The ¹H NMR data obtained for both 5 and 6 showed the absence of a resonance that could be assigned to H-12 and in both spectra the Me-17 resonance had undergone a significant upfield shift. The observation of a 1D NOESY correlation between the Me-17 resonance at δ 1.06 and the H-2 resonance at δ 5.47 showed that the major epoxide was the β

[1] Jordan, A.; Hadfield, J.A.; Lawrence, N.J.; McGowen, A.T. *Med. Res. Rev.* **1998**, *18*, 259-296.

[2] a) Giannakakou, P.; Gussio, R.; Nogales, E.; Downing, K.H.; Zaharevitz, D.; Bollbuck, B.; Poy, G.; Sackett, D.; Nicolaou, K.C.; Fojo, T. *Proc. Natl. Acad. Sci.* **2000**, *97*, 2904-2909, and b) Ojima, I; Chakravarty, S.; Inoue, T.; Lin, S.; He, L.; Horowitz, S.B.; Kuduk, S.D.; Danishefsky, S.J. *ibid* **1999**, *96*, 4256-4261, c) He, L.; Jagtap, P.G.; Kingston, D.G.I.; Shen, H.-J.; Orr, G.A.; Horowitz, S.B. *Biochemistry* **2000**, *39*, 3972-3978.

[3] Lindel, T.; Jensen, P. R.; Wasserman, A. J.; Cornell, L. A.; Fenical, W.; Long, B. H.; Casazza, A. M.; Carboni, J.; Fairchild, C. R. *J. Am. Chem. Soc.* **1997**, *119*, 8744-8745.

[4] a) Chen, X.-T.; Bhattacharya, S.K.; Zhou, B.; Gutteridge, C.E.; Pettus, T.R.R.; Danishefsky, S.J. *J. Am. Chem. Soc.* **1999**, *121*, 6563-6579, b) Nicolaou, K.C.; Ohshima, T.; Hosokawa, F.L.; van Delft, F.L.; Vourloumis, D.; Xu, J.Y.; Pfefferkorn, J.; Kim, S. *J. Am. Chem. Soc.* **1998**, *120*, 8674-8680, c) Nicolaou, K.C.; Xu, J.Y.; Kim, S.; Pfefferkorn, J.; Ohshima, T.; Vourloumis, D.; Hosokawa, S. *J. Am. Chem. Soc.* **1998**, *120*, 8661-8673, and d) Nicolaou, K.C.; Winssinger, D.; Vourloumis, D.; Ohshima, T.; Kim, S,; Pfefferkorn, J.; Xu, J.-Y.; Li, T. *J. Am. Chem. Soc.* **1998**, *120*, 10814-10826.

[5] a) Cinel, B; Roberge, M.; Behrisch, H.; van Ofwegen, L.; Castro, C. B.; Andersen, R. J. *Org. Lett.* **2000**, *2*, 257-260, b) Roberge, M.; Cinel, B.; Anderson, H.J.; Lim, L.; Jiang, X.; Xu, L.; Kelly, M.T.; Andersen, R.J. *Cancer Research* **2000**, *60*, 5052-5058, c) Britton, R.; Roberge, M.; Berisch, H.; Andersen, R.J. *Tetrahedron Lett.* **2001**, *42*, 2953 – 2956.

[6] Cinel, B.; Patrick, B. O.; Roberge, M.; Andersen, R. J. *Tet. Lett.* **2000**, *41*, 2811-2815.

isomer **5**. Treatment of **1** with SeO_2 (5 equiv.) in refluxing EtOH gave a single product **7** in modest yield.
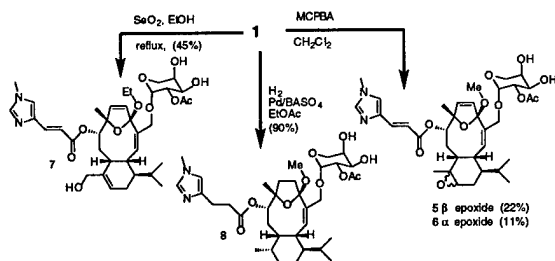
Scheme 2

Finally, we examined reduction of the olefins. A solution of **1** in EtOAc containing catalytic Pd on $BaSO_4$ was stirred at rt for 1 h under 1 atm of H_2 resulting in the formation of hexahydroeleutherobin **8** (Scheme 2). The ^1H NMR of **8** contained only a single olefinic proton resonance at δ 5.78 (d, J = 9.3 Hz), assigned to H-2, indicating that the $\Delta^{5,6}$, $\Delta^{11,12}$, and $\Delta^{2',3'}$ double bonds had been reduced. A ROESY correlation observed between the Me-17 resonance (δ 0.76 (d, J = 7.0 Hz)) and the H-2 resonance demonstrated that hydrogen had added to the β face of the $\Delta^{11,12}$ olefin. Hexahydroeleutherobin **8** (IC_{50} >10^4 nM) was found to be more than five thousand-fold less active than eleutherobin (**1**) (IC_{50} 20 nM) in a cell-based antimitotic assay,[5b] indicating that the presence of one or more of the reduced double bonds is important for tubulin binding. Biological evaluation of a synthetic sarcodictyin library had suggested that reduction of the $\Delta^{5,6}$ olefin had minimal effect on the potency of tubulin polymerization.[4d] Therefore, 5,6,11,12-tetrahydroeleutherobin (**9**) and 2',3'-dihydroeleutherobin (**10**) were selected as logical targets to further probe the biological effects of olefin reduction.
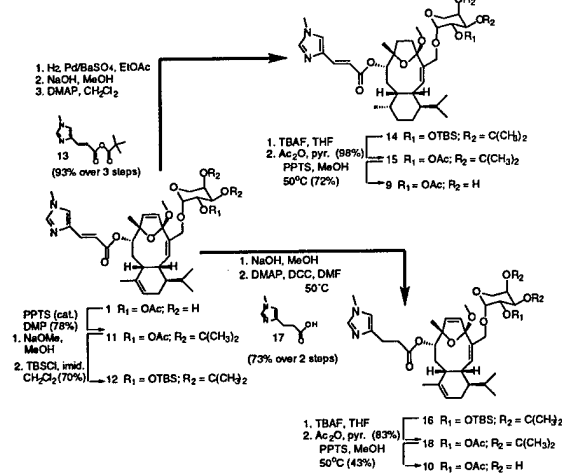
Scheme 3

The synthesis of **9** started from eleutherobin (**1**), by first forming the 3",4"-acetonide **11**, which was subsequently deacetylated to the 2" alcohol and converted directly to the 2" TBS ether **12**. Hydrogenation of **12**, using a catalytic amount of Pd on $BaSO_4$, gave the 5,6,11,12,2',3'-hexahydro derivative *vide supra* (Scheme 3). Hydrolysis of the crude

hydrogenation product cleanly cleaved the C-8 ester side chain, which was replaced with a N-methylurocanic ester residue[4c] to afford **14**. Removal of the TBS protecting group, followed by acetylation provided **15**, which was subsequently deprotected under mildly acidic conditions to give 5,6,11,12-tetrahydroeleutherobin (**9**). Similarily, 2'3'-dihydroeleutherobin (**10**) was prepared from the 2" TBS ether **12**, by hydrolysis of the N-methylurocanic ester residue (NaOH, MeOH) to provide a secondary alcohol at C-8, which was directly coupled with 2,3-dihydro-N-methylurocanic acid (**17**) using DCC and DMAP in warm (50°C) DMF to afford **16**. A deprotection/acetylation sequence similar to that employed in the synthesis of the tetrahydro derivative **9**, provided **10** in good overall yield.

The C-4 ketals **3** and **4** had antimitotic activity (IC_{50} 20 and 80 nM) comparable to eleutherobin (IC_{50} 20 nM) demonstrating that a bulky group can be tolerated at this position. The α-epoxide **6** and the 17-hydroxyeleutheside **7** had antimitotic potencies comparable to **1**, while the β-epoxide **5** was ten-fold less active (IC_{50} **5**: 300, **6**: 30, **7**: 20 nM). This was unexpected in light of the dramatic decrease in activity previously shown by caribaeoside,[5] attributed to the presence of a polar alcohol functionality in a binding region that was thought to require lipophilic character.[2b] Since hydroxylation at Me-17 and α-epoxidation at C-11/C-12 do not affect activity, the major negative effect of the C-11 OH in caribaeoside must be more subtle than originally thought.[5a]

Figure 1A shows antimitotic activity in a cell-based assay[5b] for **1**, and the synthetic derivatives **8**, **9**, and **10**. Tetrahydroeleutherobin **9** (IC_{50} 200 nM) was only ten-fold less active than eleutherobin, suggesting that reduction of the $\Delta^{2',3'}$ olefin was primarily responsible for the dramatically reduced activity of **8** (IC_{50} >10^4 nM). This was confirmed by the observation that 2',3'-dihydroeleutherobin (**10**) (IC_{50} ≈ 20,000 nM) is a thousand-fold less active than eleutherobin (**1**). The lack of activity of 2',3'-dihydroeleutherobin (**10**) in the cell-based antimitotic assay is mirrored in its complete lack of ability to promote the polymerization of purified bovine tubulin in a standard *in vitro* assay (Figure 1B).

The pharmacophore models put forward to date[2a-c] have all suggested that the C-8 urocanic ester is important for tubulin binding in the eleuthesides, however, the remarkably stringent requirement for the 2',3' double bond demonstrated here was completely unanticipated. This important feature of eleutheside binding, along with the observed tolerance for certain types of oxygenated functionality in the cyclohexane ring, will have to be accommodated in future iterations of the models.
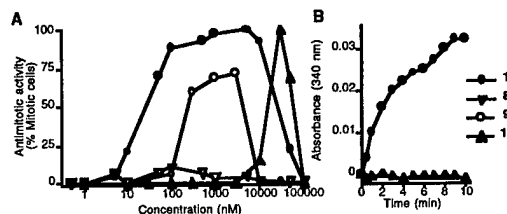

Figure 1. A, antimitotic activity of **1**, **8**, **9**, and **10**;[5b] B, microtubule-stabilizing activity of eleutherobin and 2',3'-dihydroeleutherobin.

Supporting Information. Experimental procedures for the synthetic transformations and tabulated bioactivity data (16 pages).

Diterpenoids from Cultured *Erythropodium caribaeorum*

Orazio Taglialatela-Scafati,[†§] Martha Campbell,[¥] Michel Roberge,[‡] and Raymond J. Andersen[§*]

Departments of Chemistry, EOS, Biochemistry, and Molecular Biology University of British Columbia, Vancouver, B.C. V6T 1Z1; Ocean Dreams, Inc., Tampa Bay, Florida
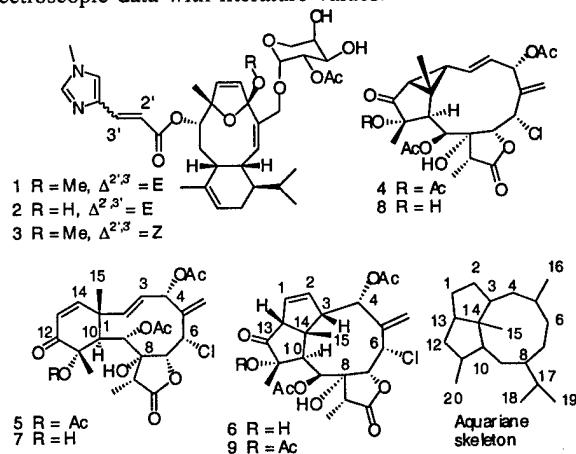
Producing an adequate and sustainable supply of compound represents one of the major challenges to developing invertebrate-derived marine natural product drug leads into clinically useful entities.[1] Harvesting invertebrate specimens from the wild is not a viable source of a drug-substance because it is environmentally unsound and it is unpredictable. The obvious and preferred solution to this supply problem is total synthesis of the natural product or simplified analogs.[2] However, many marine natural products with promising biological activity are too complex to be readily synthesized on a commercial scale[3,4] and frequently the minimal pharmacophore is also a daunting synthetic challenge.[5] Aquaculture represents an attractive intermediate solution that utilizes the biosynthetic capabilities of the source organism to generate the compound of interest in a controlled and renewable fashion. Despite the appeal of aquaculture production of bioactive natural products, the difficulties associated with growing marine invertebrates in culture has thus far limited this approach to a small number of demonstration examples.[1]

Eleutherobin (1) is a microtubule-stabilizing diterpenoid glycoside originally isolated from the rare Australian octoacoral *Eleutherobia* sp.[6] Although two elegant total syntheses of eleutherobin (1) have been reported,[4] the anticancer potential of eleutherobin has never been fully evaluated because total synthesis and the original natural source both failed to provide sufficient material for effective *in vivo* testing. Recently, it was discovered that *Erythropodium caribaeorum*, a relatively abundant Caribbean gorgonian, is a good source of eleuthesides[7] and it has provided sufficient eleutherobin (1) for preliminary animal studies[8] and chemical transformations to new analogs.[9] *E. caribaeorum* grows well in culture and it is a staple of the decorative sea-water aquarium industry. We have examined methanol extracts of cultured *E caribaeorum* to determine if these animals produce the diterpenoids found in wild animals. The extracts yielded eleutherobin (1), desmethyleleutherobin (2), Z-eleutherobin (3), erythrolide A (4),[10] and erythrolide B (5) in amounts comparable to those reported from Dominican reef animals,[7] along with aquariolide A (6), which has not been reported to date from field-harvested *E. caribaeorum*.[7,10,11] Aquariolide A (6) has an unprecedented highly rearranged diterpenoid carbon skeleton[12] that can be formally derived from the 'briarane' skeleton found in erythrolide B (5) by sequential di-π-methane and vinyl-cyclopropane rearrangements (VCR).

Aquarium-grown specimens of *E caribaeorum* (400 g wet wt.) were extracted multiple times with MeOH. Fractionation of the combined MeOH extracts via solvent partitioning, silica-gel flash chromatography, and normal-phase HPLC (Supporting Materials) gave 1 (5.0 mg), 2 (1.2 mg), 3 (0.8 mg), 4, (290 mg), 5 (1.4 g), and 6 (3.0 mg). The known compounds 1-5 were identified by comparison of their spectroscopic data with literature values.[7,10]


1 R = Me, Δ²′³ = E
2 R = H, Δ²³′ = E
3 R = Me, Δ²′³ = Z

4 R = Ac
8 R = H

5 R = Ac
7 R = H

6 R = H
9 R = Ac

Aquariane skeleton

Aquariolide A (6) was isolated as a colorless oil that gave [M⁺] and [M⁺ + 2] ions at *m/z* 496.1498 and 498.1487 (≈ 3:1) in the HREIMS consistent with a molecular formula of $C_{24}H_{29}O_9Cl$, requiring ten sites of unsaturation. One fragment of 6, stretching in a continuous sequence from the acetoxy methine at C-4 (¹H: δ 5.71) along the linear carbon chain to the methine at C-10 (¹H: δ 2.70), including the α-methyl-γ-lactone fused at C-7/C-8, was shown to be identical to the corresponding C-4 to C-10 fragment in erythrolide B (5) by detailed analysis of the 1D and 2D NMR data obtained for 6 (Supporting Materials). COSY correlations observed between H-4 (δ 5.71) and an aliphatic methine resonance at δ 3.03, assigned to H-3, identified the first point of difference between 6 and 5. Additional COSY correlations extended this spin system from H-3 through the vicinal *cis* olefinic protons H-2 (δ 5.82) and H-1 (δ 6.11) to its terminus at the aliphatic methine H-13 (δ 3.43). The H-3 resonance showed allylic coupling to H-1 and homoallylic coupling to H-13 in the COSY spectrum, consistent with the assigned spin system. With the ¹H assignments in hand, HMQC correlations permitted routine assignments of ¹³C resonances to C-3 (δ_63.1), C-2 (δ 126.8), C-1 (δ 131.5), C-13 (δ 69.4), and C-10 (δ 43.5).

A methyl singlet resonance at δ 1.60 (Me-15) showed HMBC correlations to a quaternary carbon resonance at δ 49.6 (C-14) and to the C-3, C-13, and C-10 resonances, which required that C-3, C-13 and C-10 must all be attached to the carbon (C-14) bearing the methyl group. This set of connectivities established the presence of a 9-membered ring in 6 that is fused to a cyclopentene ring at C-3 and C-14.

A second methyl singlet at δ 1.12 (Me-20) also showed HMBC correlations to the C-10 resonance (δ 43.5) and to non-protonated carbons at δ 79.6 (C-11) and 209.0 (C-12), demonstrating that the oxygenated tertiary carbon (C-11) bearing the methyl group (Me-20) was situated between C-10 and the ketone (C-12). The fragments identified above account for all of the atoms in aquariolide, except for single hydrogen that was not attached to carbon, and they account for nine of the ten sites of unsaturation. Therefore, the ketone (C-12) had to be attached to C-13 to generate a five-membered ring representing the final site of unsaturation, and the oxygen functionality at C-11 had to be an alcohol to accommodate the final hydrogen atom. The cyclpentanone ring so formed mirrors the one present in erythrolide A (4).

The relative stereochemistry of 6 was deduced from the ROESY data. All the dipolar couplings observed for the C-4 to C-12 fragment were in complete agreement with the stereochemistry reported for the same region in erythrolides A (4) and B (5). In particular, the following cross-peaks were detected: H-4/H-6; H-6/H-7; Me-18/OH-8; H-7/MeCOO-9; H-10/OH-8; H-9/Me-20; OH-11/Me-20. Transannular nOes between OH-8 and H-16a, and between H-10 and H-16b, were also detected. Analysis of molecular models revealed that 6 can readily adopt a nine-memberd ring conformation where the olefinic methylene protons H-16a and H-16b sit close to OH-8 and H-10, respectively. ROESY correlations observed between Me-15 (δ 1.60) and both H-3 (δ 3.30) and H-13 (δ 3.43) indicated a cis relationship for all of these protons. Furthermore, a ROESY correlation between H-3 (δ 3.30) and H-4 (δ 5.71), and their scalar coupling of only 3.0 Hz, were only consistent with the placement of these protons on the same face of the nine-membered ring. Fixing the H-3/H-4 relative stereochemistry correlated the relative stereochemistry of the cyclopentene ring with the remaining part of the molecule. Assuming that the C-4 to C-12 fragment of aquariolide A (6) has the same absolute configuration as the corresponding fragments in erythrolides A (4) and B (5),[10] the absolute configuration of aquariolide A is as shown in 6.

Scheme 1
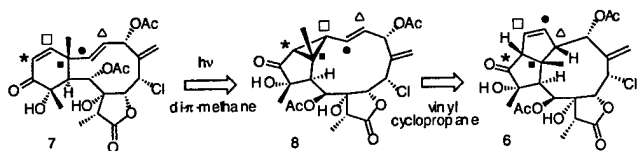
The new aquariane skeleton can be formally derived from a putative briarane precursor 7 (Scheme 1). A di-_-methane rearrangement of 7 gives an erythrane intermediate 8, which can undergo a VCR rearrangement to give the aquariane skeleton in 6. Fenical et al. showed that erythrolide B (5) can be converted to erythrolide A (4) by irradiation with ambient sunlight.[10] Although most VCR rearrangements require high temperatures, there are reports of photochemical variants.[13] Side by side exposure of solutions of erythrolide B (5) and erythrolide A (4) in MeOH, acetone,[13] and toluene[13] to ambient sunlight resulted in the expected transformation of 5 to 4 in all solvents but produced no detectable change in 4 in any of the three solvents.[14] Therefore, it seems that the VCR rearrangement required to convert an erythrane such as 8 into an aquariane (i.e. 6) must be enzyme mediated. The absence of detectable amounts of the 11-acetoxy aquariolide A analog 9 in the cultured E caribaeorum extracts supports this conclusion.

Erythrolide A (4) is a major component of the extract and if its conversion to an aquariolide occurred via a non-enzymatic photochemical process, then 9 should have been a significant component of the extractable diterpenoids.

Our finding that cultured E. caribaeorum produces significant amounts of eleuthesides opens the way to large scale aquaculture production of these interesting antimitotic agents should they prove to be viable anticancer drugs. The parallel discovery of aquariolide A (6) adds a new dimension to our understanding of the diterpenoid chemistry of E caribaeorum. It suggests that the photochemical conversion of briaranes (i.e. 5) to erythranes (i.e. 4) is not simply a tolerated happen-stance event but an integral part of the metabolic pathways of the gorgonian, since there must be enzymes that have evolved to transform erythranes (i.e. 8) into aquarianes (i.e. 6).

"Supporting Information Available:" NMR spectra, tables of NMR assignments, physical constants, and isolation details for (6). (5 pages)

† Permanent address: Dipartimento di Chimica delle Sostanze Naturali, Università degli Studi di Napoli Federico II, Via D. Montesano 49, I-80131 Napoli, Italy; § Chemistry/EOS; ‡Biochemistry/Molecular Biology; ¥Ocean Dreams

(1) (a) Munro, M.H.G.; Blunt, J.W.; Dumdei, E.J.; Hickford, S.J.H.; Lill, R.E.; Li, S.X.; Battershill, C.N.; Duckworth, A.R. J. Biotechnol. 1999, 70, 15-25, and (b) Pomponi, S.A. J. Biotechnol. 1999, 70, 5-13.

(2) for examples see: (a) Cuevas, C.; Perez, M.; Martin, M. J.; Chicharro, J. L.; Fernandez-Rivas, C.; Flores, M.; Francesch, A.; Gallego, P.; Zarzuelo, M.; de la Calle, F.; Garcia, J.; Polanco, C.; Rodriguez, I.; Manzanares, I.; Org. Lett. 2000; 2, 2545-2548 and (b) Shen, Y.; Burgoyne, D. L.; J. Org. Chem. 2002,67, 3908-3910.

(3) (a) Aicher, T.D.; Buszek, K.R.; Fang, F.G.; Forsyth, C.J.; Jung, S.H.; Kishi, Y.; Matelich, M.C.; Scola, P.M.; Spero, D.M.; Yoon, S.K. J. Am. Chem. Soc. 1992, 114, 3162-3164 .

(4) a) Nicolaou, K. C.; Ohshima, T.; Hosokawa, S.; van Delft, F. L.; Vourloumis, D.; Xu, J. Y.; Pfefferkorn, J.; Kim, S. J. Am. Chem. Soc. 1998, 120, 8674-8680, b) Chen, X.-T.; Bhattacharya, S. K.; Zhou, B.; Gutteridge, C. E.; Pettus, T. R. R.; Danishefsky, S. J. J. Am. Chem. Soc.1999, 121, 6563-6579.

(5) Towle, M.J.; Salvato, K.A.; Budrow, J.; Wels, B.F.; Kuznetsov, G.; Aalfs, K.K.; Welsh, S.; Zheng, W.J.; Seletsky, B.M.; Palme, M.H.; Habgood, G.J.; Singer, L.A.; DiPietro, L.V.; Wang, Y.; Chen, J.J.; Quincy, D.A.; Davis, A.; Yoshimatsu, K.; Kishi, Y.; Yu, M.J.; Littlefield, B.A. Cancer Res. 2001, 61, 1013-1021.

(6) Lindel, T.; Jensen, P.R.; Fenical, W.; Long, B.H.; Casazza, A.M.; Carboni, J.; Fairchild, C.R. J. Am. Chem. Soc. 1997, 119, 8744-8745.

(7) (a) Cinel, B.; Roberge, M.; Behrisch, H.; van Ofwegen, L.; Castro, C. B.; Andersen, R. J. Org. Lett. 2000, 2, 257-260, and (b) Britton, R. Roberge, M.; Berisch, H.; Andersen, R.J. Tetrahedron Lett. 2001, 42, 2953-2956.

(8) The results of these investigations will be reported elsewhere.

(9) Britton, R.; de Silva, E. D.; Bigg, C. M.; McHardy, L. M.; Roberge, M.; Andersen, R. J.; J. Am. Chem. Soc. 2001, 123, 8632-8633.

(10) Look, S.A.; Fenical, W.F.; Van Engen, D.; Clardy, J. J. Am. Chem. Soc. 1984, 106, 5026-5027.

(11) for previous chemical studies of E. caribaeorum see: (a) Banjoo, D.; Mootoo, B.S.; Ramsewak, R.S.; Sharma, R.; Lough, A.J.; McLean, S.; Reynolds, W.F. J. Nat. Prod. 2002, 65, 314-318, (b) Maharaj, D.; Pascoe, K.O.; Tinto, W.F.; J. Nat. Prod. 1999, 62, 313-314. (c) Banjoo, D.; Maxwell, A.R.; Mootoo, B.S.; Lough, A.J.; McLean, S.; Reynolds, W.F. Tetrahedron Lett. 1998, 39, 1469-1472; (d) Pathirana C.; Fenical, W.F.; Corcoran, E.; Clardy, J. Tetrahedron Lett. 1993, 34, 3371-3372, (e) Dookran, R.; Maharaj, D.; Mootoo, B.S.; Ramsewak, R.; McLean, S.; Reynolds, W.F.; Tinto, W.F. J. Nat. Prod. 1993, 56, 1051-1056, and (f) Pordesimo E.O.; Schmitz, F.J.; Ciereszko, L.S.; Hossain, M.B.; Van der Helm, D. J. Org. Chem. 1991, 56, 2344-2357.

(12) We propose the name 'aquariane' and a numbering scheme that preserves the C-4 to C-12 numbering of the briarane and erythrane skeletons.

(13) Sonawane, H.R.; Bellur, N.S.; Kulkarni, D.G.; Ahuja, J.R. *Synlett* **1993**, 875-884.

(14) This result is consistent with Fenical's report (Ref. 10) that irradiation of a benzene solution of erythrolide B (**5**) in a quartz cell with a Hg lamp gave the single product erythrolide A (**4**).

Insert Table of Contents artwork here
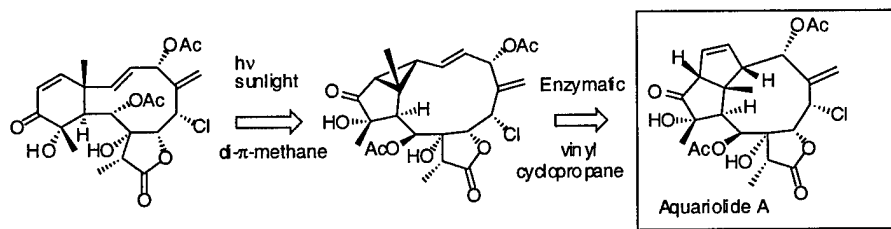
hν
sunlight

di-π-methane

Enzymatic

vinyl
cyclopropane

Aquariolide A

Producing an adequate and sustainable supply of compound represents one of the major challenges to developing invertebrate-derived marine natural product drug leads into clinically useful entities. Aquaculture represents an attractive solution that utilizes the biosynthetic capabilities of the source organism to generate the compound of interest in a controlled and renewable fashion. MeOH extracts of cultured specimens of the Caribbean gorgonian *Erythropodium caribaeorum* have been found to contain the known antimitotic eleuthesides eleutherobin (**1**), desmethyleleutherobin (**2**), and Z-eleutherobin (**3**), and the 'briarane' diterpenoids erythrolide A (**4**), and erythrolide B (**5**) in amounts comparable to those reported from wild-harvested reef animals. The cultured animals also contained the novel diterpenoid aquariolide A (**6**) that has not been reported to date from wild animals. Aquariolide A (**6**) has an unprecedented highly rearranged diterpenoid carbon skeleton that can be formally derived from the 'briarane' skeleton found in erythrolide B (**5**) by sequential di-π-methane and vinyl-cyclopropane rearrangements. The finding that cultured *E. caribaeorum* produces significant amounts of eleuthesides opens the way to large scale aquaculture production of these interesting antimitotic agents should they prove to be viable anticancer drugs. The parallel discovery of aquariolide A (**6**) suggests that the photochemical conversion of briaranes (i.e. **5**) to erythranes (i.e. **4**) is not simply a tolerated happen-stance event but an integral part of the metabolic pathways of the gorgonian, since there must be enzymes that have evolved to transform erythranes (i.e. **8**) into aquarianes (i.e. **6**).